Effect of Fluid–Structure Interaction on Vibration and Deflection Analysis of Generally Orthotropic Submerged Micro-plate with Crack Under Thermal Environment: An Analytical Approach

Shashank Soni[1] · N. K. Jain[1] · P. V. Joshi[2] · Ankur Gupta[1]

Abstract

Purpose To develop a new analytical model for vibration analysis of cracked-submerged orthotropic micro-plate affected by fibre orientation and thermal environment.

Methods The proposed analytical model is based on Kirchhoff's classical thin plate theory and the size effect is introduced using the modified couple stress theory. Effect of crack is deduced using appropriate crack compliance coefficients based on line spring model while the effect of thermal environment is introduced in terms of thermal in-plane moments and forces. The coupling of shear and normal stresses for fibre orientation is represented using the coefficient of mutual influence. The fluid forces associated with its inertial effects are added in the governing differential equation to incorporate the fluid–structure interaction effect.

Results The results are presented for frequency response as affected by different fibre orientation, crack length, crack location, level of submergence, temperature variation and material length-scale parameter for simply supported boundary condition. Furthermore, to study the phenomenon of shifting of primary resonance in a cracked micro-plate, the classical relations for central deflection of plate is also proposed.

Conclusions The results show that the fundamental frequency of micro-plate decreases by the presence of crack and thermal environment and this decrease in frequency is further intensified by the presence of surrounding fluid medium in present study. Another important conclusion is that with increase in temperature variation the reduction in frequency at 45° of fibre orientation is less when compared to 0 and 90° for both intact and cracked orthotropic plates.

Keywords Crack · Fibre orientation · Fluid · Micro-plate · Thermal environment

Shashank Soni and Ankur Gupta contributed equally.

✉ Ankur Gupta
  ankurgupta1729@gmail.com

  Shashank Soni
  shashanksoninitr@gmail.com

  N. K. Jain
  nkjmanit@rediffmail.com

  P. V. Joshi
  psad@rediffmail.com

[1] Department of Mechanical Engineering, National Institute of Technology, Raipur, Chhattisgarh 492010, India

[2] Department of Basic Sciences and Engineering, Indian Institute of Information Technology, Nagpur, Maharashtra 440006, India

Introduction

In recent decades, orthotropic plates and shells are widely used as essential structural components in marine engineering applications which expose them to work under fluidic medium of varying temperature with unwanted intensity of high vibrations. Thus, the knowledge of the vibration characteristics of such structures under fluidic medium with temperature variation is important for their reliability evaluation. It becomes more interesting to understand the effect of temperature under fluidic medium when these structures contain various flaws in the form of holes and cracks. As per the literature, it is seen that researchers have analysed the vibration problems of intact plates in the presence of thermal and fluidic environments individually. However, the studies on analysis of cracked orthotropic plates including the effect of thermal environment and fluidic medium are

_Springer

insignificant. From the literature, it is observed that the presence of irregularities in a plate makes its dynamic behaviour drastically different from that of an intact one. To find the analytical solution of cracked thin plates, researchers have used the famous line spring model (LSM). This model was originally proposed by Rice and Levy [1], their concept of the LSM was based on Kirchhoff's thin plate theory and they represented the partial crack as continuous line spring with stretching, bending and twisting compliances. Further, to simplify the line spring model, King [2] used linear algebraic equations rather than coupled integral equations and proposed a simplified line spring model. Zeng and Dai [3] employed simplified LSM in their modelling of a cracked rectangular plate to determine the stress intensity factors at the crack tips. Solecki [4] employed the Navier's solution and finite Fourier transformation technique to construct an analytical model for vibration problem of cracked isotropic plates. Liew et al. [5] investigated the upper bound solutions for fundamental frequencies of plate using the Ritz method including the domain decomposition technique. Malhotra et al. [6] performed the frequency analysis of orthotropic plate using the Rayleigh–Ritz method. They studied the variation of fundamental frequency as affected by the fibre orientation for various boundary conditions and for various orthotropic materials. Using the LSM, the first approximate mathematical model for vibration problem of cracked isotropic plates is developed by Israr et al. [7], they used the relationship between bending and tensile stresses at far sides of the plate and at the crack area to introduce the effect of crack on governing equation of an isotropic plate. They studied the variation of crack length on the frequency response of plate for different boundary conditions. By extending the work of Israr et al. [7], a new model for a partially cracked rectangular isotropic plate with variably oriented crack is developed by Ismail and Cartmell [8]. It is concluded from their work that the natural frequencies of cracked plate decreases when crack length and its orientation increases. Taking the consideration of thermal effects, Joshi et al. [9, 10] have presented an analytical solution for buckling and vibration analysis of isotropic [9] and orthotropic [10] plate with surface and internal cracks. Soni et al. [11, 12] studied the effect of fluidic medium on vibration characteristics of cracked isotropic [11] and magneto-electro-elastic (MEE) [12] plates by incorporating the inertial effect of fluids forces on previously developed models. Recently Lai and Zhang [13] studied the buckling and vibration response of orthotropic and isotropic cracked plate under thermal effects using discrete singular convolution (DSC) method. They also proposed the relation for critical buckling temperature of cracked orthotropic and isotropic plate.

The fluid–structure interaction (FSI) problems have been receiving wide attention in current decades. In the literature, it is observed that the phenomenon of fluid–structure interaction significantly influences the vibration response of a structure. The first classical approach for FSI problem was given by Lamb [14]. He employed a hypothetical approach for computing the vibration response of a circular plate coupled with fluid. The created technique was based on the evaluation of rise in kinetic energy of surrounding fluid. Muthuveerappan et al. [15] employed the experimental technique to determine the fundamental frequencies of the intact cantilever plate submerged in water. They studied the effect of plate aspect ratio and thickness ratio on the fundamental frequencies of submerged plate. To determine the fundamental frequency of plate in water from the frequency of the plate in vacuum, Kwak [16] proposed an approximation for virtual added mass incremental factor using Rayleigh's method. In the same way, to determine the fundamental frequencies of annular plate in contact with fluid, Amabili [17] used the virtual added mass approach of Kwak [16]. To study the vibration response of intact plates vibrating under fluid, Haddara and Cao [18] have given an approximate relation for the virtual added mass. Their results are investigated experimentally as well as analytically for different submergence levels and boundary conditions. Based on Sander's shell theory and FEM technique, Kerboua et al. [19] developed an analytical model for free vibration problems of isotropic plate coupled with water. It has given the ease to study the plate–fluid interaction problems. Using the Mindlin's plate hypothesis for deriving the model, Hosseini-Hashemi et al. [20] developed an analytical model for thick horizontal plates which are submerged in fluid partially and totally. Vibration problems of plates considering the effect of both crack and fluidic medium are found in few investigations (Refs. [21–23]). The effect of through-crack on the vibration characteristics of a circular plate coupled with fluid is shown in the analysis of perforated plates using the finite element method (FEM) by Liu et al. [21]. Similarly, the effect of fluidic medium and side crack on fundamental frequency of cracked circular and rectangular plates vibrating under water is given by Si et al. [22, 23] using the computational approach of FEM.

Similarly, for the effect of thermal environment on vibration problems of plates, it is seen that the presence of thermal stress decreases the stiffness of plate which results in the reduction of natural frequency. Yang and Shen [24] have given the results for natural frequency of FGM plates subjected to thermal environment. In their work, the effect of rise in temperature, boundary condition and volume fraction index are considered as input parameters and they presented the effect of these above parameters on frequency of plate using higher order theories. Jeyaraj et al. [25] worked on the computational approach-based ANSYS and SYSNOISE to find the acoustic response and vibration attributes of an isotropic plate under certain temperature variation. Continuing their work they further analysed both responses

for a composite plate including internal material damping employing laminated plate theory [26]. The analysis of vibration problems being functionally graded plates exposed to thermal heating is stated by Li et al. [27]. Three-dimensional theory of elasticity to model the FGM plates in closeness of thermal environment is employed by them. Using the finite element method, Viola et al. [28] also practised on vibration analysis of cracked composite plate. Detailed study on vibration and buckling analyses of a functionally graded plate consists of internal discontinuities in form of cracks using FEM and first-order shear deformation (FSDT) theory is carried out by Natarajan et al. [29]. They showed the outcome of increment in crack length and temperature gradient on the natural frequency of the cracked plate.

The dynamics of vibrating structures submerged in fluid is a fundamental research problem and caters the wide engineering applications from aerodynamics to biosensors. Micro-machined plates are used as biosensors, micro-resonators, actuators, atomic force microscopes (AFMs), micro-switches, etc. It has been vastly accepted that the mechanical behaviours of small-scale structures are size dependent. It is found in the literature that as the structure dimensions diminish to the order of micro-/nano-scale, the effect of structure size plays a significant role in the correct examination of such structures. According to previous laboratory research, the classical continuum theory is unable to take account of size effects in the analysis of the behaviour of micro/nano structures. Thus, over the years, non-classical theories such as nonlocal theory, strain gradient theory and modified couple stress theory have been used by researchers to study the microstructures. Since these micro-sized structures often undergo dynamic loading and are regularly subjected to external environment such as thermal environment, knowledge of vibration characteristics become important to improve upon reliability of their design. In the recent literature on investigation of microstructures, it has been established that it alters the vibration response of plate structures [30–36]. Out of different theories which dominate the size effect on the analysis of the gradient elastic plates, among them, Mindlin and Eshel [37] proposed the strain gradient theory (SGT) to analyse the effect of microstructure. They (Ref. [37]) proposed a single length-scale parameter to catch size effect of microstructure in their expanded theory. Papargyri-Beskou and Beskos [38] established a sixth-order governing equilibrium equation of force and moment on gradient elastic plate. Extending their work, Papargyri-Beskou et al. [39] practised the principle of virtual work to draft the same problem for distinct possible boundary aspects. The bending analysis of a thin isotropic rectangular plate based on the second gradient theory is performed by Mousavi and Paavola [40]. In their developed model, they considered parameter of two length scale to capture size consequence and to make the model more competent. Akgöz and Civalek

[41, 42] presented the analytical solutions for bending, vibration and buckling problems of micro-sized plates based on modified couple stress theory [41] and modified strain gradient theory [42]. In their work, they performed a detailed parametric study to demonstrate the effect of length-scale parameter, length-to-thickness ratio on buckling load, deflection, and fundamental frequencies of micro-plates. A new mathematical model for micro-plates based on the modified couple stress theory (MCST) is established by Tsiatas [43] and Tsiatas and Yiotis [44]. In their work, they examined distinct isotropic [43] and orthotropic [44] plates of numerous shapes and dimensions to figure out the effectiveness of their suggested model (MCST) in contrast with the Kirchhoff's plate model. Extending their work, Tsiatas and Yiotis [45] also studied the static, dynamic and buckling analyses of orthotropic micro-plates based on MCST and nonlocal elasticity theory. Adopting the MCST of Tsiatas [43], Yin et al. [46] likewise worked on the vibration problems of micro-plates. In their research, they used a material-scale parameter to demonstrate the size outcome of microstructure. After evaluating the results for two distinct theories (MCST and CPT), they achieved that the results attained from MCST are always greater as compared to CPT. Ebrahimi and Barati [47] worked on buckling analysis of functionally graded (FG) nanobeams using nonlocal third-order shear deformation beam theory. They studied the thermal effects on buckling response of the nanobeams subjected to various types of thermal loading. Based on Euler–Bernoulli's beam theory, Akgöz and Civalek [48] and Demir and Civalek [49] have investigated the buckling and bending behaviour of micro-beams for various types of boundary conditions. They (Ref. [48]) studied the effects of additional material length-scale parameters, material property variation function and slenderness ratio on the buckling response of FGM micro-beams and also compared the results for different non-classical theories. Extending the work of Ref. [48], Mercan and Civalek [50, 51] and Mercan et al. [52] have also analysed the buckling response of boron nitride nanotubes (BNNTs) [50], silicon carbide nanotubes (SiCNTs) [51] and nanowires (SiCNWs) [52] considering the size effect of microstructure using different size-dependent continuum theories. They determined their critical buckling load as affected by different geometrical quantities/parameters. Numanoglu et al. [53] investigated the longitudinal free vibration behaviours of nanorods based on Eringen's nonlocal theory. Effects of nonlocal parameter, attachments, boundary conditions, and length on the natural frequencies of nanorods are studied in detail in their study. In the new governing equation of motion based on Hamilton's principle, Gao and Zhang [54] used a material length scale steady to catch the size significance of microstructure. They also figure out that their outcomes for natural frequency achieved by the non-classical plate model (MCST) are greater than that of the classical plate model

for thin plates. Most recently, Gupta et al. [55] produced an analytical model for vibration problem of a partially cracked thin isotropic and functionally graded cracked micro-plate using the LSM. They used classical plate theory (CPT) in conjunction with MCST and accomplished that their outcomes for fundamental frequencies are consistently higher for modified couple stress theory. Moreover, they demonstrated the significance of fibre orientation on vibration attributes of cracked orthotropic micro-plate [56].

It is well known from the literature (Ref. [57]) that the vibration response of a submerged micro-plate is extensively influenced by fluid loading due to its inertial effects. Also, in the case of a generally orthotropic micro-plate, the stiffness can be significantly altered by varying fibre orientation which is again reflected in the vibration response. Further, the vibration response is also dependent on the external environment such as thermal environment. Thus, the aim of the present work is to combine the research in these related areas and present comprehensive effect of microstructures, thermal environment, partial crack, surrounding fluid, fibre orientation on the vibration and deflection of the generally orthotropic micro-plate.

The present non-classical model extends the work of Refs. [56, 58] and narrows down the gap in the recently developing area of vibration analysis of cracked plates by addressing the following:

1. Vibration analysis of partially cracked orthotropic submerged plate based on the Kirchhoff's thin plate theory as affected by the fibre orientation and thermal environment is proposed.
2. The proposed model is further extended for the case of orthotropic micro-plate with fibre orientation based on the non-classical modified couple stress theory.
3. The classical relation for central deflection of cracked orthotropic submerged plate which shows an important phenomenon of a shift in primary resonance due to fibre orientation, crack, temperature, and material length-scale parameter.
4. The effect of fibre orientation, level of submergence, temperature rise, material length-scale parameter, crack length and crack location on fundamental frequency as well as central deflection of cracked orthotropic submerged plate is studied in the presence of thermal environment for simply supported boundary condition.
5. The present work presents a comparison of classical plate theory and modified couple stress theory for vibration of partially cracked orthotropic micro-plate in the presence of thermal and fluidic environments.

In the present study, an analytical model has been presented for cracked orthotropic rectangular plate in light of a non-classical approach. The moment equilibrium equations

for cracked orthotropic plate are derived by taking the consideration of thermal environment and microstructure. The effect of crack is introduced in the form of additional membrane force and bending moment using the line spring model. The effect of fluidic medium is integrated in the model in the form of added virtual mass with the help of Bernoulli's equation and velocity potential function. Figure 1 shows the plate configuration in which the in-plane dimensions of the plate are taken as L_1 and L_2 in x- and y-directions separately. The plate thickness is denoted by h. Figure 2a is the length of crack at plate centre and the depth of the crack is less than the thickness. d is the offset distance between plate centre and the crack centre along the x-axis. To study the effect of various parameters such as rise in temperature, crack length, crack location, fibre orientation, material length-scale parameter and level of submergence on fundamental frequency, SSSS (all sides simply supported) boundary condition is considered in the present work. The central deflection of the cracked plate has also been studied as affected by length of crack, location of crack, fibre orientation, temperature variation and material length-scale parameter. A comparison of these results with the classical plate theory has also been established.

Governing Equation

The governing differential equation of an intact and cracked orthotropic plate under influence of thermal environment and based on the approach of classical thin plate theory has been thoroughly treated in Refs. [9, 10], respectively. In this section, a new governing equation for a partially cracked orthotropic submerged plate with various fibre orientations subjected to thermal environment is derived based on a non-classical plate theory of elasticity. The assumptions considered in the derivation are customarily according to classical plate theory for thin plates (Refs. [56, 59]).

The constitutive relations for a thin orthotropic lamina considering the temperature gradient and fibre orientation have been obtained in Ref. [60]; based on the assumptions taken in the present study, such relations for an orthotropic lamina with uniform temperature rise can be given as

$$
\left.
\begin{aligned}
\mathcal{E}_x &= \frac{\sigma_x}{E_x} - \vartheta_y \frac{\sigma_y}{E_y} - m_x \tau_{xy} + \alpha_x \Delta T \\
\mathcal{E}_y &= -\vartheta_x \frac{\sigma_x}{E_x} + \frac{\sigma_y}{E_y} - m_y \tau_{xy} + \alpha_y \Delta T \\
\gamma_{xy} &= -m_x \sigma_x - m_y \sigma_y + \frac{\tau_{xy}}{G_{xy}} + \alpha_{xy} \Delta T
\end{aligned}
\right\},
\tag{1}
$$

where $\mathcal{E}_x$, $\mathcal{E}_y$ and γ_{xy} are the mid-plane strains. $E_x, E_y, G_{xy}, \vartheta_x$ and ϑ_y are the elastic constants. α_x, α_y and α_{xy} are the thermal

Fig. 1 **a** Partially cracked orthotropic submerged plate showing fibre orientation. **b** Plate configuration showing offset distance 'd'
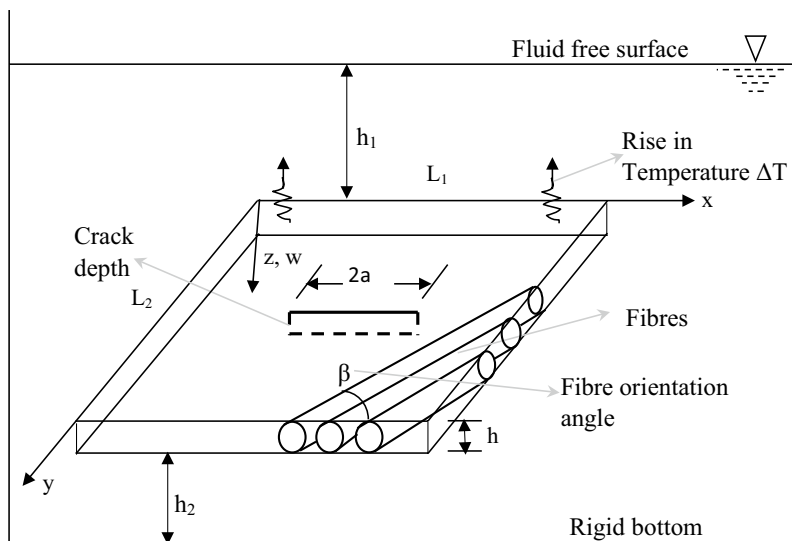
(a) Partially cracked orthotropic submerged plate showing fibre orientation
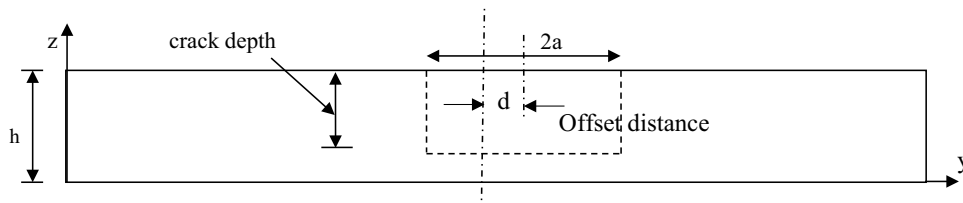
(b) Plate configuration showing offset distance 'd'

expansion coefficients. The expressions for coefficient of thermal expansion can be stated as

$$\left.\begin{array}{l} \alpha_x = \alpha_1\cos^2\beta + \alpha_2\sin^2\beta \\ \alpha_y = \alpha_1\sin^2\beta + \alpha_2\cos^2\beta \\ \alpha_{xy} = (2\sin\beta\cos\beta)(\alpha_1 - \alpha_2) \end{array}\right\}, \tag{2}$$

where m_x and m_y are the coefficients of mutual influence which depends on the material elastic constants and fibre orientation angle and represents the coupling of the shear and normal stresses. The relations for the coefficients of mutual influence can be stated as [60]

$$\left.\begin{array}{l} m_x = \sin2\beta\left\{\dfrac{\vartheta_x}{E_x} + \dfrac{1}{E_y} - \dfrac{1}{2G_{xy}} - \left(\cos^2\beta\right)\left(\dfrac{1}{E_x} + \dfrac{2\vartheta_x}{E_x} + \dfrac{1}{E_y} - \dfrac{1}{G_{xy}}\right)\right\} \\[3mm] m_y = \sin2\beta\left\{\dfrac{\vartheta_x}{E_x} + \dfrac{1}{E_y} - \dfrac{1}{2G_{xy}} - \left(\sin^2\beta\right)\left(\dfrac{1}{E_x} + \dfrac{2\vartheta_x}{E_x} + \dfrac{1}{E_y} - \dfrac{1}{G_{xy}}\right)\right\} \end{array}\right\}, \tag{3}$$

where m_x and m_y will vanish for fibre orientations $\beta = 0°$ and $\beta = 90°$ and, therefore, for the fibre orientations $\beta = 0°$ and $90°$, there is no extensional shear coupling [60]. For other than these fibre orientations, there exist six elasticity moduli:

$E_1, E_2, E_x, E_y, G_{12}, G_{xy}$. The representation of these elasticity constants can be found in Refs. [56, 60].

The mid-surface strains in the terms of transverse deflection can be stated as

$$\left.\begin{array}{l} E_x = -z\dfrac{\partial^2 w}{\partial x^2} \\[3mm] E_y = -z\dfrac{\partial^2 w}{\partial y^2} \\[3mm] \tau_{xy} = G_{xy}(-2z)\dfrac{\partial^2 w}{\partial x\partial y} \end{array}\right\}. \tag{4}$$

Using Eqs. (1)–(4), the relationship for the normal stresses (σ_x, σ_y) and the in-plane shear stress (τ_{xy}) can be written as
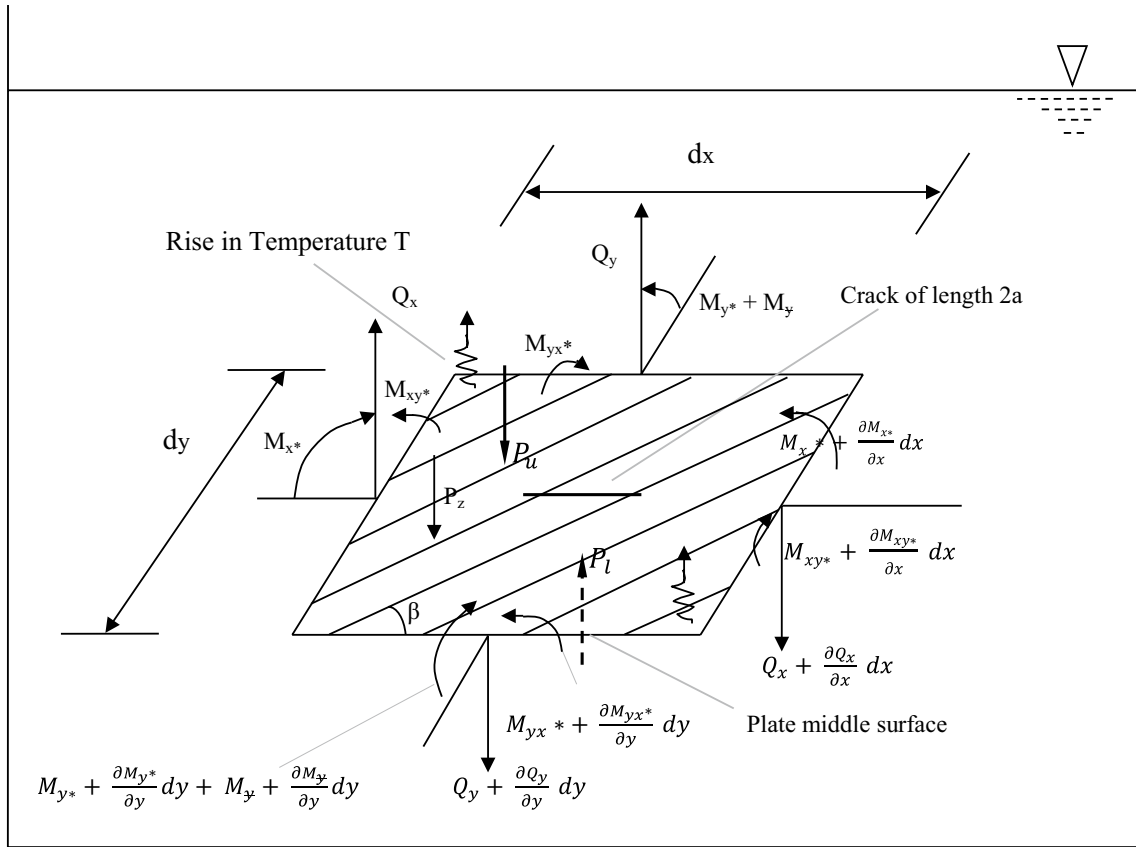
Fig. 2 Submerged orthotropic plate element showing moments and internal forces on the mid-plane

$$
\sigma_x = \frac{\begin{aligned}&\frac{E_x}{(1-\vartheta_x\vartheta_y)}\left(-z\frac{\partial^2 w}{\partial x^2}-\vartheta_y\frac{\partial^2 w}{\partial y^2}\right)+\frac{E_x(\vartheta_y m_y+m_x)}{(1-\vartheta_x\vartheta_y)\left(\frac{1}{G_{xy}}-m_y^2 E_y\right)}\left(-2z\frac{\partial^2 w}{\partial x\partial y}-m_y E_y z\frac{\partial^2 w}{\partial y^2}\right)\\[2mm]&-\frac{E_x}{(1-\vartheta_x\vartheta_y)}\left(\frac{(\vartheta_y m_y+m_x)(\alpha_{xy}\Delta T+m_y E_y\alpha_y\Delta T)}{\left(\frac{1}{G_{xy}}-m_y^2 E_y\right)}+(\alpha_x+\alpha_y\vartheta_y)\Delta T\right)\end{aligned}}{1-\frac{E_x(\vartheta_y m_y+m_x)}{(1-\vartheta_x\vartheta_y)\left(\frac{1}{G_{xy}}-m_y^2 E_y\right)}\left(m_x+m_y\vartheta_x\frac{E_y}{E_x}\right)},
\tag{5}
$$

$$
\sigma_y = \frac{\begin{aligned}&\frac{E_y}{(1-\vartheta_x\vartheta_y)}\left(-z\frac{\partial^2 w}{\partial y^2}-\vartheta_x\frac{\partial^2 w}{\partial x^2}\right)+\frac{E_y(\vartheta_x m_x+m_y)}{(1-\vartheta_x\vartheta_y)\left(\frac{1}{G_{xy}}-m_x^2 E_x\right)}\left(-2z\frac{\partial^2 w}{\partial x\partial y}-m_x E_x z\frac{\partial^2 w}{\partial x^2}\right)\\[2mm]&-\frac{E_y}{(1-\vartheta_x\vartheta_y)}\left(\frac{(\vartheta_x m_x+m_y)(\alpha_{xy}\Delta T+m_x E_x\alpha_x\Delta T)}{\left(\frac{1}{G_{xy}}-m_x^2 E_x\right)}+(\alpha_x\vartheta_x+\alpha_y)\Delta T\right)\end{aligned}}{1-\frac{E_y(\vartheta_x m_x+m_y)}{(1-\vartheta_x\vartheta_y)\left(\frac{1}{G_{xy}}-m_x^2 E_x\right)}\left(m_y+m_x\vartheta_y\frac{E_x}{E_y}\right)},
\tag{6}
$$

$$\tau_{xy} = \dfrac{-2z\dfrac{\partial^2 w}{\partial x \partial y} + \dfrac{1}{\left(1-\vartheta_x\vartheta_y\right)}\left[m_x E_x\left(-z\dfrac{\partial^2 w}{\partial x^2} - \vartheta_y z \dfrac{\partial^2 w}{\partial y^2}\right) + m_y E_y\left(-z\dfrac{\partial^2 w}{\partial y^2} - \vartheta_x z \dfrac{\partial^2 w}{\partial x^2}\right)\right] - \dfrac{\Delta T\left(\alpha_{xy} + m_x E_x\left(\alpha_x + \alpha_y \vartheta_y\right) + m_y E_y\left(\alpha_y + \alpha_x \vartheta_x\right)\right)}{\left(1-\vartheta_x\vartheta_y\right)}}{\dfrac{1}{G_{xy}} - \dfrac{m_x E_x\left(\vartheta_y m_y + m_x\right) + m_y E_y\left(\vartheta_x m_x + m_y\right)}{\left(1-\vartheta_x\vartheta_y\right)}}. \tag{7}$$

On integrating Eqs. (5)–(7) over the plate thickness, we obtain the expressions for bending and twisting moments as

$$\left. \begin{aligned} M_x &= \int_{-h/2}^{h/2} \sigma_x z \, \mathrm{d}z \\[6pt] M_y &= \int_{-h/2}^{h/2} \sigma_y z \, \mathrm{d}z \\[6pt] M_{xy} &= \int_{-h/2}^{h/2} \tau_{xy} z \, \mathrm{d}z \end{aligned} \right\}, \tag{8}$$

$$M_x = \dfrac{-D_x\left\{\left(\dfrac{\partial^2 w}{\partial x^2} + \vartheta_y \dfrac{\partial^2 w}{\partial y^2}\right) + \dfrac{\left(\vartheta_y m_y + m_x\right)}{\dfrac{1}{G_{xy}} - m_y^2 E_y}\left(2\dfrac{\partial^2 w}{\partial x \partial y} + m_y E_y \dfrac{\partial^2 w}{\partial y^2}\right)\right\}}{1 - \dfrac{E_x\left(\vartheta_y m_y + m_x\right)}{\left(1-\vartheta_x\vartheta_y\right)\left(\dfrac{1}{G_{xy}} - m_y^2 E_y\right)}\left(m_x + m_y \vartheta_x \dfrac{E_y}{E_x}\right)} - M_{Tx}, \tag{9}$$

$$M_y = \dfrac{-D_y\left\{\left(\dfrac{\partial^2 w}{\partial y^2} + \vartheta_x \dfrac{\partial^2 w}{\partial x^2}\right) + \dfrac{\left(\vartheta_x m_x + m_y\right)}{\dfrac{1}{G_{xy}} - m_x^2 E_x}\left(2\dfrac{\partial^2 w}{\partial y \partial x} + m_x E_x \dfrac{\partial^2 w}{\partial x^2}\right)\right\}}{1 - \dfrac{E_y\left(\vartheta_x m_x + m_y\right)}{\left(1-\vartheta_x\vartheta_y\right)\left(\dfrac{1}{G_{xy}} - m_x^2 E_x\right)}\left(m_y + m_x \vartheta_y \dfrac{E_x}{E_y}\right)} - M_{Ty}, \tag{10}$$

$$M_{xy} = \dfrac{-\left\{\dfrac{h^3}{6}\dfrac{\partial^2 w}{\partial x \partial y} + \left(D_x m_x + \vartheta_x D_y m_y\right)\dfrac{\partial^2 w}{\partial x^2} + \left(D_y m_y + \vartheta_y D_x m_x\right)\dfrac{\partial^2 w}{\partial y^2}\right\}}{\dfrac{1}{G_{xy}} - \dfrac{m_x E_x\left(\vartheta_y m_y + m_x\right) + m_y E_y\left(\vartheta_x m_x + m_y\right)}{\left(1-\vartheta_x\vartheta_y\right)}} - M_{Txy}, \tag{11}$$

where

$$M_{Tx} = \int_{-h/2}^{h/2} \dfrac{\dfrac{E_x}{\left(1-\vartheta_x\vartheta_y\right)}\left(\dfrac{\left(\vartheta_y m_y + m_x\right)\left(\alpha_{xy}\Delta T + m_y E_y \alpha_y \Delta T\right)}{\left(\dfrac{1}{G_{xy}} - m_y^2 E_y\right)} + \left(\alpha_x + \alpha_y \vartheta_y\right)\Delta T\right)}{1 - \dfrac{E_x\left(\vartheta_y m_y + m_x\right)}{\left(1-\vartheta_x\vartheta_y\right)\left(\dfrac{1}{G_{xy}} - m_y^2 E_y\right)}\left(m_x + m_y \vartheta_x \dfrac{E_y}{E_x}\right)} z \, \mathrm{d}z,$$

$$M_{Ty} = \int_{-h/2}^{h/2} \dfrac{\dfrac{E_y}{\left(1-\vartheta_x\vartheta_y\right)}\left(\dfrac{\left(\vartheta_x m_x + m_y\right)\left(\alpha_{xy}\Delta T + m_x E_x \alpha_x \Delta T\right)}{\left(\dfrac{1}{G_{xy}} - m_x^2 E_x\right)} + \left(\alpha_x \vartheta_x + \alpha_y\right)\Delta T\right)}{1 - \dfrac{E_y\left(\vartheta_x m_x + m_y\right)}{\left(1-\vartheta_x\vartheta_y\right)\left(\dfrac{1}{G_{xy}} - m_x^2 E_x\right)}\left(m_y + m_x \vartheta_y \dfrac{E_x}{E_y}\right)} z \, \mathrm{d}z,$$

$$M_{Txy} = \int_{-h/2}^{h/2} \dfrac{\dfrac{\Delta T\left(\alpha_{xy} + m_x E_x\left(\alpha_x + \alpha_y \vartheta_y\right) + m_y E_y\left(\alpha_y + \alpha_x \vartheta_x\right)\right)}{\left(1-\vartheta_x\vartheta_y\right)}}{\dfrac{1}{G_{xy}} - \dfrac{m_x E_x\left(\vartheta_y m_y + m_x\right) + m_y E_y\left(\vartheta_x m_x + m_y\right)}{\left(1-\vartheta_x\vartheta_y\right)}} z \, \mathrm{d}z.$$

In the above equations, M_x, M_y and M_{xy} are the internal bending and twisting moments and M_{Tx}, M_{Ty} and M_{Txy} are bending and twisting moments due to thermal environment.

Consider a cracked orthotropic submerged plate element as shown in Fig. 2. The internal forces and bending moments acting on the mid-plane of the plate are considered as per Kirchhoff's plate theory [59]. M_{y*}, M_{x*} and $M_{xy*} = M_{yx*}$ denote the bending moments and twisting moments. M_{-y} represents the additional bending moment due to the crack (Refs. [61, 62]).

On resolving the internal forces along the z-direction and taking moment about x- and y-directions, we get the following equilibrium equations:

$$\sum F_z = 0,$$

$$\frac{\partial Q_x}{\partial x} + \frac{\partial Q_y}{\partial y} = \rho h \frac{\partial^2 w}{\partial t^2} + \Delta P - p_z, \tag{12}$$

where Q_x and Q_y are the transverse forces. $\rho h \frac{\partial^2 w}{\partial t^2}$ denotes the inertia force of vibrating plate. ΔP is the fluid dynamic pressure difference between the upper (P_u) and lower (P_l) surfaces of the plate. ρ and h are the density and thickness of plate and p_z represents the transverse load per unit area.
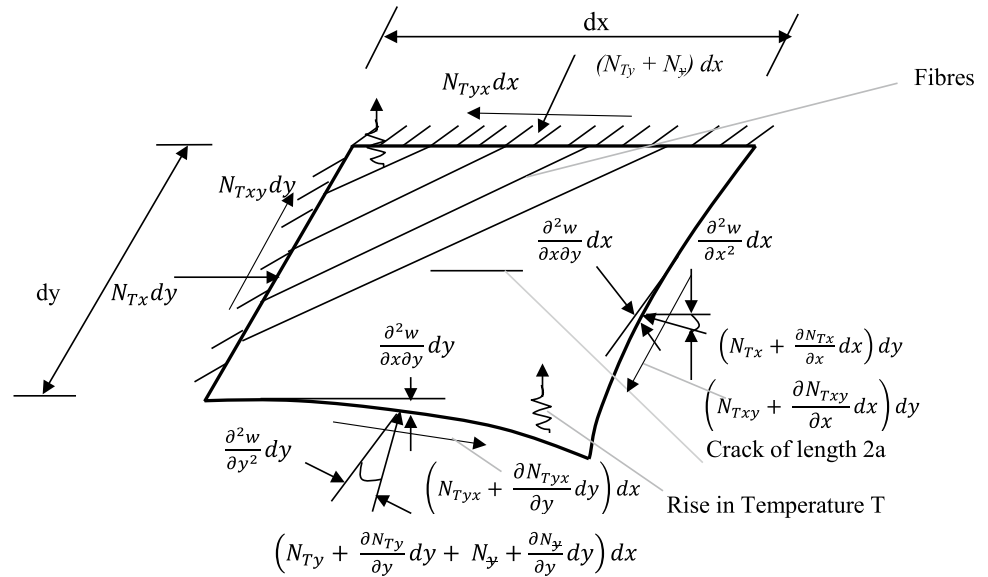
Taking moment equilibrium about the *x*- and *y*-axis one obtains

$$\frac{\partial M_{y*}}{\partial y} + \frac{\partial M_{xy*}}{\partial x} + \frac{\partial M_{y}}{\partial y} = Q_y, \tag{13}$$

$$\frac{\partial M_{x*}}{\partial x} + \frac{\partial M_{yx*}}{\partial y} = Q_x, \tag{14}$$

where

$$M_{x*} = M_x + M_x^l, \tag{15}$$

$$M_{y*} = M_y + M_y^l, \tag{16}$$

$$M_{xy*} = M_{xy} + M_{xy}^l, \tag{17}$$

where M_y^l, M_x^l and $M_{xy}^l = M_{yx}^l$ are the extra bending and twisting moments per unit length due to the effect of microstructure. The detailed description for Eqs. (15)–(17), addition of M_x^l, M_y^l and M_{xy}^l to internal bending and twisting moments (M_x, M_y and M_{xy}) based on the modified couple stress theory can be referred in Appendix A.

From Eqs. (12), (13) and (14), one obtains

$$\frac{\partial^2 M_{x*}}{\partial x^2} + 2\frac{\partial^2 M_{xy*}}{\partial x\partial y} + \frac{\partial^2 M_{y*}}{\partial y^2} + \frac{\partial^2 M_{y}}{\partial y^2} = \rho h\frac{\partial^2 w}{\partial t^2} + \Delta P - p_z. \tag{18}$$

On expressing the bending and twisting moments of Eq. (18) in terms of transverse deflection from Eq. (8) to Eq. (11), the governing equation of cracked orthotropic micro-plate can be given as

$$\frac{(D_x + D^{lx})\left\{ \left(\frac{\partial^4 w}{\partial x^4} + \vartheta_y\frac{\partial^4 w}{\partial x^2\partial y^2}\right) + \frac{(\vartheta_y m_y + m_x)}{\frac{1}{G_{xy}} - m_y^2 E_y}\left(2\frac{\partial^4 w}{\partial x^3\partial y} + m_y E_y\frac{\partial^4 w}{\partial x^2\partial y^2}\right) \right\}}{1 - \frac{E_x(\vartheta_y m_y + m_x)}{(1-\vartheta_x\vartheta_y)\left(\frac{1}{G_{xy}} - m_y^2 E_y\right)}\left(m_x + m_y\vartheta_x\frac{E_y}{E_x}\right)}$$

$$+ \frac{2\left\{\frac{h^3}{6}\frac{\partial^4 w}{\partial x^2\partial y^2} + \left((D_x + D^{lx})m_x + \vartheta_x(D_y + D^{ly})m_y\right)\frac{\partial^4 w}{\partial x^3\partial y} + \left((D_y + D^{ly})m_y + \vartheta_y(D_x + D^{lx})m_x\right)\frac{\partial^4 w}{\partial y^3\partial x} \right\}}{\frac{1}{G_{xy}} - \frac{m_x E_x(\vartheta_y m_y + m_x) + m_y E_y(\vartheta_x m_x + m_y)}{(1-\vartheta_x\vartheta_y)}}$$

$$+ \frac{(D_y + D^{ly})\left\{ \left(\frac{\partial^4 w}{\partial y^4} + \vartheta_x\frac{\partial^4 w}{\partial x^2\partial y^2}\right) + \frac{(\vartheta_x m_x + m_y)}{\frac{1}{G_{xy}} - m_x^2 E_x}\left(2\frac{\partial^4 w}{\partial y^3\partial x} + m_x E_x\frac{\partial^4 w}{\partial x^2\partial y^2}\right) \right\}}{1 - \frac{E_y(\vartheta_x m_x + m_y)}{(1-\vartheta_x\vartheta_y)\left(\frac{1}{G_{xy}} - m_x^2 E_x\right)}\left(m_y + m_x\vartheta_y\frac{E_x}{E_y}\right)}$$

$$= -\rho h\frac{\partial^2 w}{\partial t^2} - \Delta P + p_z - \frac{\partial^2 M_{Tx}}{\partial x^2} - \frac{\partial^2 M_{Ty}}{\partial y^2} - \frac{\partial^2 M_{Txy}}{\partial x\partial y} + \frac{\partial^2 M_{y}}{\partial y^2}, \tag{19}$$

where $D_x = \frac{E_x h^3}{12(1-\vartheta_x \vartheta_y)}$ and $D_y = \frac{E_y h^3}{12(1-\vartheta_x \vartheta_y)}$ are the flexural rigidities of an orthotropic plate in x- and y-directions and $D_x = \frac{E_x l^2 h}{2(1+\vartheta_x)}$ and $D_y = \frac{E_y l^2 h}{2(1+\vartheta_y)}$ are the additional flexural/ bending rigidities due to the microstructure.

The in-plane forces considered for the cracked orthotropic plate are shown in Fig. 3. It is well known from the literature (Refs. [9, 10]) that the in-plane forces produced by the transverse deflection introduces non-linearity to the governing equation but does not affect the plate's stiffness. In this present work, the in-plane forces induced only due to temperature variation are considered. Taking the summation of the in-plane forces along z-axis, we get

$$\sum F_z(x, y) = -N_{Tx}\frac{\partial^2 w}{\partial x^2} - N_{Ty}\frac{\partial^2 w}{\partial y^2} - 2N_{Txy}\frac{\partial^2 w}{\partial x \partial y} - N_{\overline{y}}\frac{\partial^2 w}{\partial y^2}, \tag{20}$$

where N_{Tx}, N_{Ty} and N_{Txy} represent the in-plane compressive forces due to the uniform temperature rise of plate and N_y is the additional in-plane force due to the line crack [7, 9, 10]. On adding the in-plane forces given by Eq. (20) in Eq. (19), the governing equation of the cracked orthotropic plate considering the effect of couple stress, fibre orientation and thermal environment can be stated as

plane of the plate and replacing the constraints due to the net ligament by some bending and membrane stresses on the crack location. Israr et al. [7] proposed the relationship of tensile and bending stresses at far edges of plate and at crack tips for an isotropic plate. These relations were further modified and applied to a specially orthotropic plate by Joshi et al. [63]. Extending their work Joshi et al. [9] have also derived the above relationship in the presence of temperature variation for the isotropic plates. Similar relations for the partially cracked orthotropic plate incorporating the moments and in-plane forces due to temperature variation and internal microstructure can be presented as

$$M_{\overline{y}} = -\frac{2a}{3\left(\frac{\alpha_{bt}}{6} + \alpha_{bb}\right)(3+\vartheta_x)(1-\vartheta_x)h + 2a} M_{y*}, \tag{22}$$

$$N_{\overline{y}} = \frac{2a}{(6\alpha_{bt} + \alpha_{tt})(1-\vartheta_x^2)h + 2a} N_{Ty}, \tag{23}$$

where the terms $\alpha_{tt}, \alpha_{bb}, \alpha_{bt} = \alpha_{tb}$ are crack compliance coefficients for stretching, bending and tensile bending, respectively. These coefficients depend on crack depth (d) to thickness (h) ratio and vanish when d = 0. The required expressions for compliance coefficients as a function of

$$\frac{(D_x + D^{lx})\left\{\left(\frac{\partial^4 w}{\partial x^4} + \vartheta_y \frac{\partial^4 w}{\partial x^2 \partial y^2}\right) + \frac{(\vartheta_y m_y + m_x)}{\frac{1}{G_{xy}} - m_y^2 E_y}\left(2\frac{\partial^4 w}{\partial x^3 \partial y} + m_y E_y \frac{\partial^4 w}{\partial x^2 \partial y^2}\right)\right\}}{1 - \frac{E_x(\vartheta_y m_y + m_x)}{(1-\vartheta_x \vartheta_y)\left(\frac{1}{G_{xy}} - m_y^2 E_y\right)}\left(m_x + m_y \vartheta_x \frac{E_y}{E_x}\right)}$$

$$+ \frac{2\left\{\begin{array}{c}\frac{h^3}{6}\frac{\partial^4 w}{\partial x^2 \partial y^2} + (D^{lx})m_x + \vartheta_x(D_y + D^{ly})m_y)\frac{\partial^4 w}{\partial x^3 \partial y} + \\ ((D_y + D^{ly})m_y + \vartheta_y(D_x + D^{lx})m_x)\frac{\partial^4 w}{\partial y^3 \partial x}\end{array}\right\}}{\frac{1}{G_{xy}} - \frac{m_x E_x(\vartheta_y m_y + m_x) + m_y E_y(\vartheta_x m_x + m_y)}{(1-\vartheta_x \vartheta_y)}}$$

$$+ \frac{(D_y + D^{ly})\left\{\left(\frac{\partial^4 w}{\partial y^4} + \vartheta_x \frac{\partial^4 w}{\partial x^2 \partial y^2}\right) + \frac{(\vartheta_x m_x + m_y)}{\frac{1}{G_{xy}} - m_x^2 E_x}\left(2\frac{\partial^4 w}{\partial y^3 \partial x} + m_x E_x \frac{\partial^4 w}{\partial x^2 \partial y^2}\right)\right\}}{1 - \frac{E_y(\vartheta_x m_x + m_y)}{(1-\vartheta_x \vartheta_y)\left(\frac{1}{G_{xy}} - m_x^2 E_x\right)}\left(m_y + m_x \vartheta_y \frac{E_x}{E_y}\right)}$$

$$= -\rho h \frac{\partial^2 w}{\partial t^2} - \Delta P - \frac{\partial^2 M_{Tx}}{\partial x^2} - \frac{\partial^2 M_{Ty}}{\partial y^2} + \frac{\partial^2 M_y}{\partial y^2} - N_{Tx}\frac{\partial^2 w}{\partial x^2} - N_{Ty}\frac{\partial^2 w}{\partial y^2} - 2N_{Txy}\frac{\partial^2 w}{\partial x \partial y} - N_{\overline{y}}\frac{\partial^2 w}{\partial y^2} + P_z. \tag{21}$$

Crack Terms

The crack terms (m_y and r_y) are obtained using Line Spring Model (LSM) given by Rice and Levy [1]. The LSM can convert a complicated surface crack problem into a plane strain one and bring the net ligament stresses to the neutral

crack depth to plate thickness ratio ($\delta = d/h$) can be written as (Ref. [7])

$$\begin{aligned}\alpha_{tt} = 1.154\delta^2[&1.98 - 0.54\delta + 18.65\delta^2 - 33.70\delta^3 \\ &+ 99.26\delta^4 - 211.90\delta^5 + 436.84\delta^6 \\ &- 460.48\delta^7 + 289.98\delta^8],\end{aligned}$$

$$\alpha_{bb} = 1.154\delta^2[1.98 - 3.28\delta + 14.43\delta^2 - 31.26\delta^3$$
$$+ 63.56\delta^4 - 103.36\delta^5 + 147.52\delta^6$$
$$- 127.69\delta^7 + 61.50\delta^8],$$

$$\alpha_{bt} = \alpha_{tb} = 1.154\delta^2[1.98 - 1.91\delta + 16.01\delta^2 - 34.84\delta^3$$
$$+ 83.93\delta^4 - 153.65\delta^5 + 256.72\delta^6$$
$$- 244.67\delta^7 + 133.55\delta^8].$$

It is to be noted that these above expressions for compliance coefficients are valid only for $(\delta = d/h)$ values within the range 0.1–0.7 and in the present model, δ is taken 0.6.

To introduce the effect of location of crack on frequency under thermal environment, the values of the above crack compliance coefficients is to be multiplied by a factor $\left(2/\sqrt{\pi\left(\frac{\gamma}{\Gamma}\right)}\right)\exp\left(-\left(\frac{(\Gamma-\xi_c)^2 L_1^2}{\left(\frac{\gamma}{\Gamma}\right)}\right)\right)$, here $\xi_c = d/L_1$ is the eccentricity ratio, d is the offset distance between centre of the crack and centre of the plate, $\gamma = (h/L_1)$ and $\Gamma = (a/L_1)$. Similar treatment to introduce the effect of crack location can be found in the work of Bose et al. [64] and Gupta et al. [56, 61, 62]. Hence, the effect of change in crack location is taken into consideration by suitably modifying the crack compliance coefficients.

Fluid Terms

Consider a cracked plate element submerged in fluid horizontally as shown in Fig. 1. On expressing the velocity potential function in terms of Laplace equation and then using Bernoulli's equation for the fluid dynamic pressure at fluid–plate interaction, we obtained the following expressions for the dynamic pressure acting on the plate's upper surface (P_u) and lower surface (P_l) as [19] (the detailed derivation for fluid modelling can be referred from Appendix B)

$$P_u = -\frac{\rho_f}{\mu}\left[\frac{1 + Ce^{2\mu h_1}}{1 - Ce^{2\mu h_1}}\right]\frac{\partial^2 w}{\partial t^2}, \tag{24}$$

$$P_l = -\frac{\rho_f}{\mu}\left[\frac{1 + e^{-2\mu h_2}}{1 - e^{-2\mu h_2}}\right]\frac{\partial^2 w}{\partial t^2}, \tag{25}$$

where $C = \frac{g_a\mu - \omega^2}{g_a\mu - \omega^2}$ in which ω denotes the frequency of wave motion at free surface of fluid and g_a is the acceleration due to gravity. ρ_f is fluid density per unit volume and μ is plane wavenumber which is taken as independent of boundary condition and it can be determined as $\mu = \pi\sqrt{\frac{1}{L_1^2} + \frac{1}{L_2^2}}$ (Refs. [19, 11]). The approximate value of $C = -1$ is taken in the present work to avoid the influence of non-linearity on plate–fluid interface (Ref. [19]). Here $\frac{\partial^2 w}{\partial t^2}$ represents the inertia of the surrounding fluid that forces it to oscillate when the plate vibrates. h_1 is the height of fluid above the surface of plate whereas h_2 is the level of fluid below the plate surface.

For fully submerged plate, the net fluid dynamic pressure can be determined using Eqs. (18) and (19). The resulting fluid dynamic pressure difference (ΔP) for the submerged plate can given as

$$\Delta P = P_u - P_l = -\frac{\rho_f}{\mu}\left[\frac{1 + Ce^{2\mu h_1}}{1 - Ce^{2\mu h_1}} - \frac{1 + e^{-2\mu h_2}}{1 - e^{-2\mu h_2}}\right]\frac{\partial^2 w}{\partial t^2}, \tag{26}$$

$$\Delta P = m_{add}\frac{\partial^2 w}{\partial t^2}, \tag{27}$$

where $m_{add} = -\frac{\rho_f}{\mu}\left[\frac{1 + Ce^{2\mu h_1}}{1 - Ce^{2\mu h_1}} - \frac{1 + e^{-2\mu h_2}}{1 - e^{-2\mu h_2}}\right]$ is the additional virtual mass of submerged plate due to surrounding fluid. Thus, for the case of submerged plate vibrations, the mass of the plate is increased due to a layer of fluid vibrating with the plate. This added mass is referred to as virtual added mass.

On employing Eqs. (22), (23) and (27) in Eq. (21) and stating the moments M_y^* in terms of transverse deflection (w), from Eqs. (16) and (10) we get the required governing equation of motion of cracked orthotropic plate as

$$
\begin{aligned}
&\frac{(D_x + D^{lx})\left\{ \left(\frac{\partial^4 w}{\partial x^4} + \vartheta_y \frac{\partial^4 w}{\partial x^2 \partial y^2} \right) + \frac{(\vartheta_y m_y + m_x)}{\frac{1}{G_{xy}} - m_y^2 E_y} \left(2\frac{\partial^4 w}{\partial x^3 \partial y} + m_y E_y \frac{\partial^4 w}{\partial x^2 \partial y^2} \right) \right\}}{1 - \frac{E_x(\vartheta_y m_y + m_x)}{(1 - \vartheta_x \vartheta_y)\left(\frac{1}{G_{xy}} - m_y^2 E_y \right)} \left(m_x + m_y \vartheta_x \frac{E_y}{E_x} \right)} \\
&+ \frac{2\left\{ \begin{array}{c} \frac{h^3}{6}\frac{\partial^4 w}{\partial x^2 \partial y^2} + \left((D_x + D^{lx})m_x + \vartheta_x (D_y + D^{ly})m_y \right)\frac{\partial^4 w}{\partial x^3 \partial y} + \\ \left((D_y + D^{ly})m_y + \vartheta_y (D_x + D^{lx})m_x \right)\frac{\partial^4 w}{\partial y^3 \partial x} \end{array} \right\}}{\frac{1}{G_{xy}} - \frac{m_x E_x(\vartheta_y m_y + m_x) + m_y E_y(\vartheta_x m_x + m_y)}{(1 - \vartheta_x \vartheta_y)}} \\
&+ \frac{(D_y + D^{ly})\left\{ \left(\frac{\partial^4 w}{\partial y^4} + \vartheta_x \frac{\partial^4 w}{\partial x^2 \partial y^2} \right) + \frac{(\vartheta_x m_x + m_y)}{\frac{1}{G_{xy}} - m_x^2 E_x} \left(2\frac{\partial^4 w}{\partial y^3 \partial x} + m_x E_x \frac{\partial^4 w}{\partial x^2 \partial y^2} \right) \right\}}{1 - \frac{E_y(\vartheta_x m_x + m_y)}{(1 - \vartheta_x \vartheta_y)\left(\frac{1}{G_{xy}} - m_x^2 E_x \right)} \left(m_y + m_x \vartheta_y \frac{E_x}{E_y} \right)} = -(\rho h + m_{add})\frac{\partial^2 w}{\partial t^2} \\
&+ \frac{2a}{3\left(\frac{\alpha_{bt}}{6} + \alpha_{bb} \right)(3 + \vartheta_x)(1 - \vartheta_x)h + 2a} \left[\frac{(D_y + D^{ly})\left\{ \left(\frac{\partial^4 w}{\partial y^4} + \vartheta_x \frac{\partial^4 w}{\partial x^2 \partial y^2} \right) + \frac{(\vartheta_x m_x + m_y)}{\frac{1}{G_{xy}} - m_x^2 E_x} \left(2\frac{\partial^4 w}{\partial y^3 \partial x} + m_x E_x \frac{\partial^4 w}{\partial x^2 \partial y^2} \right) \right\}}{1 - \frac{E_y(\vartheta_x m_x + m_y)}{(1 - \vartheta_x \vartheta_y)\left(\frac{1}{G_{xy}} - m_x^2 E_x \right)} \left(m_y + m_x \vartheta_y \frac{E_x}{E_y} \right)} + \frac{\partial^4 M_{Ty}}{\partial y^4} \right] \\
&- N_{Tx}\frac{\partial^2 w}{\partial x^2} - 2N_{Txy}\frac{\partial^2 w}{\partial x \partial y} - \frac{(1 + 2a)}{(6\alpha_{bt} + \alpha_{tt})(1 - \nu_x^2)h + 2a}N_{Ty}\frac{\partial^2 w}{\partial y^2} - \frac{\partial^2 M_{Tx}}{\partial x^2} - \frac{\partial^2 M_{Ty}}{\partial y^2} + P_z.
\end{aligned}
\tag{28}
$$

Solution of Governing Equation

The presence of external environment-like rise in temperature has been included in the governing differential equation of cracked orthotropic submerged plate in the form of thermal bending moments and in-plane compressive forces. The present work restricts itself to the solution of governing equation for the case of uniformly heated plates ($M_{Tx} = M_{Ty} = 0$). Since, in majority of engineering applications thin plate structures having good thermal conductivity are used, there is a little temperature gradient along the plate thickness and they can be considered as uniformly heated plates. The constant in-plane compressive forces arising due to temperature are only considered for making the model geometrically linear. The modal functions which depend on the boundary conditions can be selected for the general solution of governing equation as

$$
w(x, y, t) = \sum_{n=1}^{\infty} \sum_{m=1}^{\infty} A_{mn} X_m Y_n \emptyset_{mn}(t).
\tag{29}
$$

In the above equation, X_m and Y_n are the modal functions which depend on the boundary conditions of the cracked plate under the fluidic medium, A_{mn} is arbitrary amplitude and $\emptyset_{mn}(t)$ is the time-dependent modal term. The modal functions X_m and Y_n for the two boundary conditions considered in this work can be found from the literature (Refs. [7, 9, 10]). For uniform heating of the plate, the constant in-plane forces in terms of lateral deflection can be stated as [10]

$$
\left.
\begin{aligned}
N_{Tx} &= \frac{E_x \Delta T h}{(1 - \vartheta_x \vartheta_y)} \left(\frac{(\vartheta_y m_y + m_x)(\alpha_{xy} + m_y E_y \alpha_y)}{\left(\frac{1}{G_{xy}} - m_y^2 E_y \right)} + (\alpha_x + \alpha_y \vartheta_y) \right) \\
N_{Ty} &= \frac{E_y \Delta T h}{(1 - \vartheta_x \vartheta_y)} \left(\frac{(\vartheta_x m_x + m_y)(\alpha_{xy} + m_x E_x \alpha_x)}{\left(\frac{1}{G_{xy}} - m_x^2 E_x \right)} + (\alpha_x + \alpha_x \vartheta_y) \right) \\
N_{Txy} &= \frac{\Delta T h(\alpha_{xy} + m_x E_x(\alpha_x + \alpha_y + \vartheta_y) + m_y E_y(\alpha_y + \alpha_x + \vartheta_x))}{(1 - \vartheta_x \vartheta_y)}
\end{aligned}
\right\}.
\tag{30}
$$

On substituting Eqs. (29) and (30) in Eq. (28) and multiplying Eq. (28) by $X_m Y_n$ and then integrating over whole plate area, the governing equation of submerged orthotropic cracked plate considering the thermal effects can be written as

$$
\left(\rho h + m_{\text{add}}\right) \sum_{n=1}^{\infty} \sum_{m=1}^{\infty} A_{mn} \int_{0}^{L1} \int_{0}^{L2} X_m^2 Y_n^2 \mathrm{d}x\mathrm{d}y \frac{\partial^2 \emptyset_{mn}(t)}{\partial t^2}
$$

$$
+ \sum_{n=1}^{\infty} \sum_{m=1}^{\infty} A_{mn}\emptyset_{mn}(t) \int_{0}^{L1} \int_{0}^{L2} \left\{ \frac{(D_x + D^{lx})\left\{ \left(X_m^{iv}Y_n + \vartheta_y X_m^{ii}y_n^{ii}\right) + \frac{(\vartheta_y m_y + m_x)}{\frac{1}{G_{xy}} - m_y^2 E_y}\left(2X_m^{iii}y_n^i + m_y E_y X_m^{ii}y_n^{ii}\right) \right\}}{1 - \frac{E_x(\vartheta_y m_y + m_x)}{(1-\vartheta_x\vartheta_y)\left(\frac{1}{G_{xy}} - m_y^2 E_y\right)}\left(m_x + m_y \vartheta_x \frac{E_y}{E_x}\right)} \right.
$$

$$
+ \frac{2\left\{ \frac{h^3}{6}X_m^{ii}y_n^{ii} + \left((D_x + D^{lx})m_x + \vartheta_x(D_y + D^{ly})m_y\right)X_m^{iii}y_n^i + \left((D_y + D^{ly})m_y + \vartheta_y(D_x + D^{lx})m_x\right)X_m^i y_n^{iii} \right\}}{\frac{1}{G_{xy}} - \frac{m_x E_x(\vartheta_y m_y + m_x) + m_y E_y(\vartheta_x m_x + m_y)}{(1-\vartheta_x\vartheta_y)}}
$$

$$
+ \frac{(D_y + D^{ly})\left\{ \left(Y_n^{iv}X_m + \vartheta_x X_m^{ii}y_n^{ii}\right) + \frac{(\vartheta_x m_x + m_y)}{\frac{1}{G_{xy}} - m_x^2 E_x}\left(2X_m^i y_n^{iii} + m_x E_x X_m^{ii}y_n^{ii}\right) \right\}}{1 - \frac{E_y(\vartheta_x m_x + m_y)}{(1-\vartheta_x\vartheta_y)\left(\frac{1}{G_{xy}} - m_x^2 E_x\right)}\left(m_y + m_x \vartheta_y \frac{E_x}{E_y}\right)}
$$

$$
- \frac{2a}{3\left(\frac{\alpha_{bt}}{6} + \alpha_{bb}\right)(3+\vartheta_x)(1-\vartheta_x)h + 2a} \frac{(D_y + D^{ly})\left\{ \left(Y_n^{iv}X_m + \vartheta_x X_m^{ii}y_n^{ii}\right) + \frac{(\vartheta_x m_x + m_y)}{\frac{1}{G_{xy}} - m_x^2 E_x}\left(2X_m^i y_n^{iii} + m_x E_x X_m^{ii}y_n^{ii}\right) \right\}}{1 - \frac{E_y(\vartheta_x m_x + m_y)}{(1-\vartheta_x\vartheta_y)\left(\frac{1}{G_{xy}} - m_x^2 E_x\right)}\left(m_y + m_x \vartheta_y \frac{E_x}{E_y}\right)}
$$

$$
+ \frac{E_x \Delta Th}{(1-\vartheta_x\vartheta_y)}\left(\frac{(\vartheta_y m_y + m_x)(\alpha_{xy} + m_y E_y \alpha_y)}{\left(\frac{1}{G_{xy}} - m_y^2 E_y\right)} + (\alpha_x + \alpha_y \vartheta_y) \right)X_m^{ii}Y_n
$$

$$
+ \left(1 + \frac{2a}{(6\alpha_{bt} + \alpha_{tt})(1-\vartheta_x^2)h + 2a}\right)\frac{E_y \Delta Th}{(1-\vartheta_x\vartheta_y)}\left(\frac{(\vartheta_x m_x + m_y)(\alpha_{xy} + m_x E_x \alpha_x)}{\left(\frac{1}{G_{xy}} - m_x^2 E_x\right)} + (\alpha_x \vartheta_x + \alpha_y) \right)Y_n^{ii}X_m
$$

$$
+ 2\left(\frac{\Delta Th\left(\alpha_{xy} + m_x E_x(\alpha_x + \alpha_y \vartheta_y) + m_y E_y(\alpha_y + \alpha_x \vartheta_x)\right)}{(1-\vartheta_x\vartheta_y)} \right)X_m^i y_n^i \left. \right\} X_m Y_n \mathrm{d}x\mathrm{d}y = p_z. \tag{31}
$$

On neglecting the point load p_z for free vibration analysis, Eq. (31) can be expressed in the form of famous Duffing equation as

$$
M_{mn}\frac{\partial^2 \emptyset_{mn}(t)}{\partial t^2} + K_{mn}\emptyset_{mn}(t) = 0, \tag{32}
$$

where

$$
M_{mn} = \left(\rho h + m_{\text{add}}\right) \sum_{n=1}^{\infty} \sum_{m=1}^{\infty} A_{mn} \int_{0}^{L1} \int_{0}^{L2} X_m^2 Y_n^2 \mathrm{d}x\mathrm{d}y, \tag{33}
$$

$$
\begin{aligned}
K_{mn} = \sum_{n=1}^{\infty} \sum_{m=1}^{\infty} A_{mn} \emptyset_{mn}(t) \int_{0}^{L1} \int_{0}^{L2} & \left\{ \frac{(D_x + D^{lx}) \left\{ \left(X_m^{iv} Y_n + \vartheta_y X_m^{ii} y_n^{ii} \right) + \frac{(\vartheta_y m_y + m_x)}{\frac{1}{G_{xy}} - m_y^2 E_y} \left(2 X_m^{iii} y_n^i + m_y E_y X_m^{ii} y_n^{ii} \right) \right\}}{1 - \frac{E_x(\vartheta_y m_y + m_x)}{(1 - \vartheta_x \vartheta_y)\left(\frac{1}{G_{xy}} - m_y^2 E_y \right)} \left(m_x + m_y \vartheta_x \frac{E_y}{E_x} \right)} \right. \\
& + \frac{2 \left\{ \frac{h^3}{6} X_m^{ii} y_n^{ii} + \left((D_x + D^{lx}) m_x + \vartheta_x (D_y + D^{ly}) m_y \right) X_m^{iii} y_n^i + \left((D_y + D^{ly}) m_y + \vartheta_y (D_x + D^{lx}) m_x \right) X_m^i y_n^{iii} \right\}}{\frac{1}{G_{xy}} - \frac{m_x E_x(\vartheta_y m_y + m_x) + m_y E_y(\vartheta_x m_x + m_y)}{(1 - \vartheta_x \vartheta_y)}} \\
& + \frac{(D_y + D^{ly}) \left\{ \left(Y_n^{iv} X_m + \vartheta_x X_m^{ii} y_n^{ii} \right) + \frac{(\vartheta_x m_x + m_y)}{\frac{1}{G_{xy}} - m_x^2 E_x} \left(2 X_m^i y_n^{iii} + m_x E_x X_m^{ii} y_n^{ii} \right) \right\}}{1 - \frac{E_y(\vartheta_x m_x + m_y)}{(1 - \vartheta_x \vartheta_y)\left(\frac{1}{G_{xy}} - m_x^2 E_x \right)} \left(m_y + m_x \vartheta_y \frac{E_x}{E_y} \right)} \\
& - \frac{2a}{3\left(\frac{\alpha_{bt}}{6} + \alpha_{bb} \right)(3 + \vartheta_x)(1 - \vartheta_x)h + 2a} \frac{(D_y + D^{ly}) \left\{ \left(Y_n^{iv} X_m + \vartheta_x X_m^{ii} y_n^{ii} \right) + \frac{(\vartheta_x m_x + m_y)}{\frac{1}{G_{xy}} - m_x^2 E_x} \left(2 X_m^i y_n^{iii} + m_x E_x X_m^{ii} y_n^{ii} \right) \right\}}{1 - \frac{E_y(\vartheta_x m_x + m_y)}{(1 - \vartheta_x \vartheta_y)\left(\frac{1}{G_{xy}} - m_x^2 E_x \right)} \left(m_y + m_x \vartheta_y \frac{E_x}{E_y} \right)} \\
& + \frac{E_x \Delta T h}{(1 - \vartheta_x \vartheta_y)} \left(\frac{(\vartheta_y m_y + m_x)(\alpha_{xy} + m_y E_y \alpha_y)}{\left(\frac{1}{G_{xy}} - m_y^2 E_y \right)} + (\alpha_x + \alpha_y \vartheta_y) \right) X_m^{ii} Y_n \\
& + \left(1 + \frac{2a}{(6\alpha_{bt} + \alpha_{tt})(1 - \vartheta_x^2)h + 2a} \right) \frac{E_y \Delta T h}{(1 - \vartheta_x \vartheta_y)} \left(\frac{(\vartheta_x m_x + m_y)(\alpha_{xy} + m_x E_x \alpha_x)}{\left(\frac{1}{G_{xy}} - m_x^2 E_x \right)} + (\alpha_x \vartheta_x + \alpha_y) \right) Y_n^{ii} X_m \\
& \left. + 2 \left(\frac{\Delta T h \left(\alpha_{xy} + m_x E_x (\alpha_x + \alpha_y \vartheta_y) + m_y E_y (\alpha_y + \alpha_x \vartheta_x) \right)}{(1 - \vartheta_x \vartheta_y)} \right) X_m^i y_n^i \right\} X_m Y_n \, dx \, dy.
\end{aligned}
\tag{34}
$$

From Eq. (32), the fundamental frequency can be obtained as $\omega_{mn}^2 = K_{mn}/M_{mn}$.

Relation for Central Deflection of Plate

Consider a cracked orthotropic submerged plate with all sides simply supported, subjected to a lateral uniformly distributed dynamic load (P_z) harmonically varying with time. For a plate in the absence of thermal moments ($M_{Tx} = M_{Ty} = M_{Txy} = 0$) and the presence of constant in-plane forces (N_{Tx} and N_{Ty}) due to thermal environment only [Eq. (30)], the governing equation (28) becomes

Table 1 Comparison of frequency parameter for intact and cracked orthotropic plate in vacuum

Frequency parameter $\left(\rho h \omega_{mn}^2 L_1^4 / \sqrt{D_x D_y}\right)$							
Length-scale parameter (l)	Fibre angle (β)	Intact		Cracked			
		$a=0$ m		$a=0.01$ m		$a=0.05$ m	
		Present	Ref. [56]	Present	Ref. [56]	Present	Ref. [56]
$l=0$ m (CPT)	0	20.03	20.03	19.89	19.89	19.59	19.59
	15	21.85	21.85	21.61	21.61	21.21	21.21
	30	25.08	25.08	24.84	24.84	24.46	24.46
	45	26.55	26.55	26.32	26.32	25.93	25.93
	60	25.08	25.08	24.83	24.83	24.34	24.34
	75	21.85	21.85	21.41	21.41	20.44	20.44
	90	20.03	20.03	18.86	18.86	15.94	15.94
$l=0.001$ m (MCST)	0	20.48	20.48	20.33	20.33	20.02	20.02
	15	22.16	22.16	21.91	21.91	21.50	21.50
	30	25.31	25.31	25.05	25.05	24.67	24.67
	45	26.75	26.75	26.51	26.51	26.12	26.12
	60	25.31	25.31	25.05	25.05	24.55	24.55
	75	22.16	22.16	21.71	21.71	20.72	20.72
	90	20.48	20.48	19.27	19.27	16.28	16.28

$L_1/L_2=1$, $\Delta T=0$

Table 2 Comparison of fundamental frequency parameter $\left(\omega_{mn} L_1^4 \sqrt{\rho h/D}\right)$ for cracked isotropic plate as a function of fluid level and half crack length. ($l=0$, $\Delta T=0$)

B.C.	Half crack length (a) (m)	Horizontally submerged in water					
		$\frac{h_1}{L_1}=0.1$		$\frac{h_1}{L_1}=0.2$		$\frac{h_1}{L_1}=0.3$	
		Present	Ref. [11]	Present	Ref. [11]	Present	Ref. [11]
SSSS	0.00	8.773	8.773	8.123	8.123	7.826	7.826
	0.01	8.554	8.554	7.921	7.921	7.631	7.631
	0.05	8.073	8.073	7.475	7.475	7.201	7.201
	0.10	7.806	7.806	7.228	7.228	6.963	6.963
CCSS	0.00	12.598	12.598	11.666	11.666	11.239	11.239
	0.01	12.243	12.243	11.337	11.337	10.922	10.922
	0.05	11.455	11.455	10.607	10.607	10.219	10.219
	0.10	11.016	11.016	10.200	10.200	9.827	9.827

SSSS all sides simply supported, *CCSS* two adjacent edges clamped and the other two simply supported

$$
\frac{(D_x + D^{lx})\left\{ \left(\frac{\partial^4 w}{\partial x^4} + \vartheta_y \frac{\partial^4 w}{\partial x^2 \partial y^2} \right) + \frac{(\vartheta_y m_y + m_x)}{\frac{1}{G_{xy}} - m_y^2 E_y} \left(2 \frac{\partial^4 w}{\partial x^3 \partial y} + m_y E_y \frac{\partial^4 w}{\partial x^2 \partial y^2} \right) \right\}}{1 - \frac{E_x(\vartheta_y m_y + m_x)}{(1 - \vartheta_x \vartheta_y)\left(\frac{1}{G_{xy}} - m_y^2 E_y \right)} \left(m_x + m_y \vartheta_x \frac{E_y}{E_x} \right)}
$$

$$
+ \frac{2\left\{ \frac{h^3}{6} \frac{\partial^4 w}{\partial x^2 \partial y^2} + \left((D_x + D^{lx})m_x + \vartheta_x (D_y + D^{ly})m_y \right) \frac{\partial^4 w}{\partial x^3 \partial y} + \left((D_y + D^{ly})m_y + \vartheta_y (D_x + D^{lx})m_x \right) \frac{\partial^4 w}{\partial y^3 \partial x} \right\}}{\frac{1}{G_{xy}} - \frac{m_x E_x (\vartheta_y m_y + m_x) + m_y E_y (\vartheta_x m_x + m_y)}{(1 - \vartheta_x \vartheta_y)}}
$$

$$
+ \frac{(D_y + D^{ly})\left\{ \left(\frac{\partial^4 w}{\partial y^4} + \vartheta_x \frac{\partial^4 w}{\partial x^2 \partial y^2} \right) + \frac{(\vartheta_x m_x + m_y)}{\frac{1}{G_{xy}} - m_x^2 E_x} \left(2 \frac{\partial^4 w}{\partial y^3 \partial x} + m_x E_x \frac{\partial^4 w}{\partial x^2 \partial y^2} \right) \right\}}{1 - \frac{E_y(\vartheta_x m_x + m_y)}{(1 - \vartheta_x \vartheta_y)\left(\frac{1}{G_{xy}} - m_x^2 E_x \right)} \left(m_y + m_x \vartheta_y \frac{E_x}{E_y} \right)}
$$

$$
- \frac{2a}{3\left(\frac{\alpha_{bt}}{6} + \alpha_{bb} \right)(3 + \vartheta_x)(1 - \vartheta_x)h + 2a} \frac{(D_y + D^{ly})\left\{ \left(\frac{\partial^4 w}{\partial y^4} + \vartheta_x \frac{\partial^4 w}{\partial x^2 \partial y^2} \right) + \frac{(\vartheta_x m_x + m_y)}{\frac{1}{G_{xy}} - m_x^2 E_x} \left(2 \frac{\partial^3 w}{\partial y^2 \partial x} + m_x E_x \frac{\partial^4 w}{\partial x^2 \partial y^2} \right) \right\}}{1 - \frac{E_y(\vartheta_x m_x + m_y)}{(1 - \vartheta_x \vartheta_y)\left(\frac{1}{G_{xy}} - m_x^2 E_x \right)} \left(m_y + m_x \vartheta_y \frac{E_x}{E_y} \right)} \tag{35}
$$

$$
+ \frac{E_x \Delta Th}{(1 - \vartheta_x \vartheta_y)} \left(\frac{(\vartheta_y m_y + m_x)(\alpha_{xy} + m_y E_y \alpha_y)}{\left(\frac{1}{G_{xy}} - m_y^2 E_y \right)} + (\alpha_x + \alpha_y \vartheta_y) \right) \frac{\partial^2 w}{\partial x^2}
$$

$$
+ \frac{E_y \Delta Th}{(1 - \vartheta_x \vartheta_y)} \left(1 + \frac{2a}{(6\alpha_{bt} + \alpha_{tt})(1 - \vartheta_x^2)h + 2a} \right) \left(\frac{(\vartheta_x m_x + m_y)(\alpha_{xy} + m_x E_x \alpha_x)}{\left(\frac{1}{G_{xy}} - m_x^2 E_x \right)} + (\alpha_x \vartheta_x + \alpha_y) \right) \frac{\partial^2 w}{\partial y^2}
$$

$$
+ 2\left(\frac{\Delta Th(\alpha_{xy} + m_x E_x(\alpha_x + \alpha_y \vartheta_y) + m_y E_y(\alpha_y + \alpha_x \vartheta_x))}{(1 - \vartheta_x \vartheta_y)} \right) \frac{\partial^2 w}{\partial x \partial y} + (\rho h + m_{\text{add}}) \frac{\partial^2 w}{\partial t^2} = P_z.
$$

Assuming the solution for lateral deflection as

$$
w(x, y, t) = W_{mn} \sin\left(\frac{m\pi x}{L_1} \right) \sin\left(\frac{n\pi y}{L_2} \right) \sin(\omega t), \tag{36}
$$

where ω is the vibrational frequency. Now for the case of forced vibrations, the applied lateral dynamic load $P_z = P_z(x, y, t)$ can be expressed as

$$
P_z(x, y, t) = P_{mn} \sin\left(\frac{m\pi x}{L_1} \right) \sin\left(\frac{n\pi y}{L_2} \right) \sin(\emptyset t), \tag{37}
$$

with $\emptyset$ being the forcing frequency of the load. Substituting the general solution of lateral deflection (w) from Eq. (34)

with ω being replaced by $\emptyset$ and the lateral dynamic load (P_z) from Eq. (35) into the governing equation (33) results in an expression for W_{mn}. Thus, the classical relation for central deflection of cracked orthotropic submerged plate subjected to uniform heating can be proposed as

$$
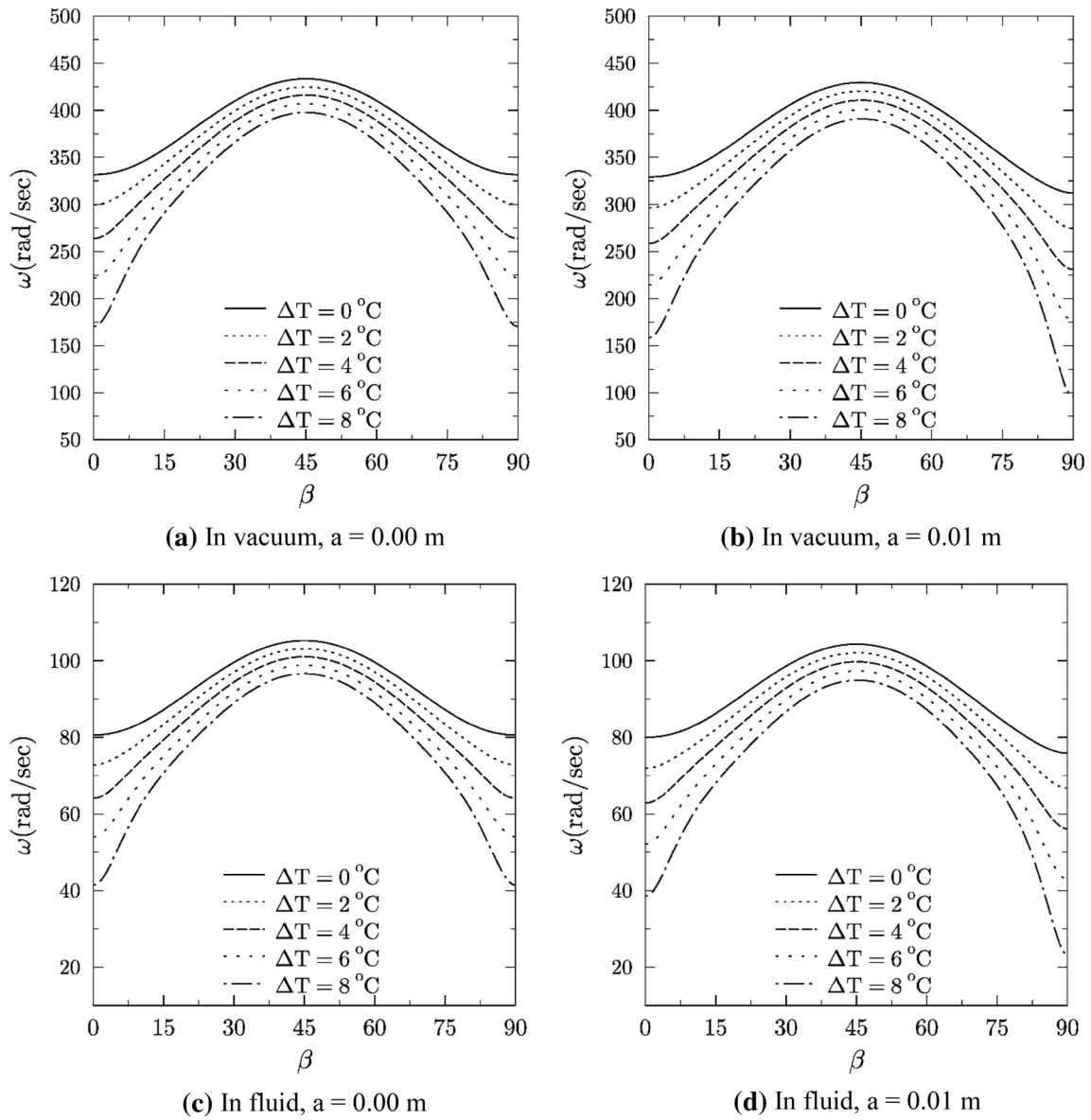W_{mn} = \frac{P_{mn}}{I - C - T - (\rho h + m_{add})\emptyset^2}, \tag{38}
$$

Fig. 4 Fundamental frequency (rad/s) as affected by temperature (ΔT) for various fibre orientations ($\beta°$) ($l = 0.001$ m, for in fluid—$h_1/L_1 = 0.1$)

where

$$I = \frac{-(D_x + D^{lx})\pi^4 \left\{ \left(\left(\frac{m}{L_1}\right)^4 + \vartheta_y \left(\frac{m}{L_1}\right)^2 \left(\frac{n}{L_2}\right)^2 \right) - \frac{(\vartheta_y m_y + m_x)}{\frac{1}{G_{xy}} - m_y^2 E_y} \left(2\left(\frac{m}{L_1}\right)^3 \left(\frac{n}{L_2}\right) - m_y E_y \left(\frac{m}{L_1}\right)^2 \left(\frac{n}{L_2}\right)^2 \right) \right\}}{1 - \frac{E_x(\vartheta_y m_y + m_x)}{(1-\vartheta_x\vartheta_y)\left(\frac{1}{G_{xy}} - m_y^2 E_y\right)} \left(m_x + m_y \vartheta_x \frac{E_y}{E_x} \right)}$$

$$+ \frac{-2\pi^4 \left\{ \begin{array}{l} \frac{h^3}{6}\left(\frac{m}{L_1}\right)^2\left(\frac{n}{L_2}\right)^2 - \left((D_x+D^{lx})m_x + \vartheta_x(D_y+D^{ly})m_y\right)\left(\frac{m}{L_1}\right)^3\left(\frac{n}{L_2}\right) \\ - \left((D_y+D^{ly})m_y + \vartheta_y(D_x+D^{lx})m_x\right)\left(\frac{m}{L_1}\right)\left(\frac{n}{L_2}\right)^3 \end{array} \right\}}{\frac{1}{G_{xy}} - \frac{m_x E_x(\vartheta_y m_y + m_x) + m_y E_y(\vartheta_x m_x + m_y)}{(1-\vartheta_x\vartheta_y)}}$$

$$+ \frac{-(D_y+D^{ly})\pi^4\left\{ \left(\left(\frac{n}{L_2}\right)^4 + \vartheta_x\left(\frac{m}{L_1}\right)^2\left(\frac{n}{L_2}\right)^2 \right) + \frac{(\vartheta_x m_x + m_y)}{\frac{1}{G_{xy}} - m_x^2 E_x}\left(-2\left(\frac{m}{L_1}\right)\left(\frac{n}{L_2}\right)^3 + m_x E_x\left(\frac{m}{L_1}\right)^2\left(\frac{n}{L_2}\right)^2 \right) \right\}}{1 - \frac{E_y(\vartheta_x m_x + m_y)}{(1-\vartheta_x\vartheta_y)\left(\frac{1}{G_{xy}} - m_x^2 E_x\right)}\left(m_y + m_x \vartheta_y \frac{E_x}{E_y} \right)}$$

$$C = \frac{2a}{3\left(\frac{\alpha_{bt}}{6} + \alpha_{bb}\right)(3+\vartheta_x)(1-\vartheta_x)h + 2a} - \frac{(D_y+D^{ly})\pi^4 \left\{ \begin{array}{l} \left(\left(\frac{n}{L_2}\right)^4 + \vartheta_x\left(\frac{m}{L_1}\right)^2\left(\frac{n}{L_2}\right)^2 \right) \\ + \frac{(\vartheta_x m_x + m_y)}{\frac{1}{G_{xy}} - m_x^2 E_x}\left(\begin{array}{l} -2\left(\frac{m}{L_1}\right)\left(\frac{n}{L_2}\right)^3 \\ +m_x E_x\left(\frac{m}{L_1}\right)^2\left(\frac{n}{L_2}\right)^2 \end{array} \right) \end{array} \right\}}{1 - \frac{E_y(\vartheta_x m_x + m_y)}{(1-\vartheta_x\vartheta_y)\left(\frac{1}{G_{xy}} - m_x^2 E_x\right)}\left(m_y + m_x \vartheta_y \frac{E_x}{E_y} \right)}$$

$$T = \pi^2 \left[\left(\frac{E_x \Delta Th}{1-v_x v_y}\left(\frac{(\vartheta_y m_y + m_x)(\alpha_{xy} + m_y E_y \alpha_y)}{\left(\frac{1}{G_{xy}} - m_y^2 E_y\right)} + (\alpha_x + \alpha_y \vartheta_y) \right) \right)\left(\frac{m}{L_1}\right)^2 + \frac{E_y \Delta Th}{1-v_x v_y}\left(1 + \frac{2a}{\left(6\alpha_{bt} + \alpha_{tt}\right)\left(1-\vartheta_x^2\right)h + 2a} \right) \right.$$

$$\left. \left(\frac{(\vartheta_x m_x + m_y)(\alpha_{xy} + m_x E_x \alpha_x)}{\left(\frac{1}{G_{xy}} - m_x^2 E_x\right)} + (\alpha_x \vartheta_x + \alpha_y) \right)\left(\frac{n}{L_2}\right)^2 - 2\left(\frac{\Delta Th\left(\alpha_{xy} + m_x E_x(\alpha_x + \alpha_y \vartheta_y) + m_y E_y(\alpha_y + \alpha_x \vartheta_x)\right)}{(1-\vartheta_x\vartheta_y)} \right)\left(\frac{m}{L_1}\right)\left(\frac{n}{L_2}\right) \right].$$

For a special case of a square plate with side L_1 and $m = n = 1$, the central deflection W_{11} takes the form which clearly shows the presence of crack (C_{11}) and temperature (T_{11}) terms:

$$W_{11} = \frac{P_{11}}{I_{11} - C_{11} - T_{11} - \left(\rho h + m_{\mathrm{add}}\right)\emptyset^2}, \tag{39}$$
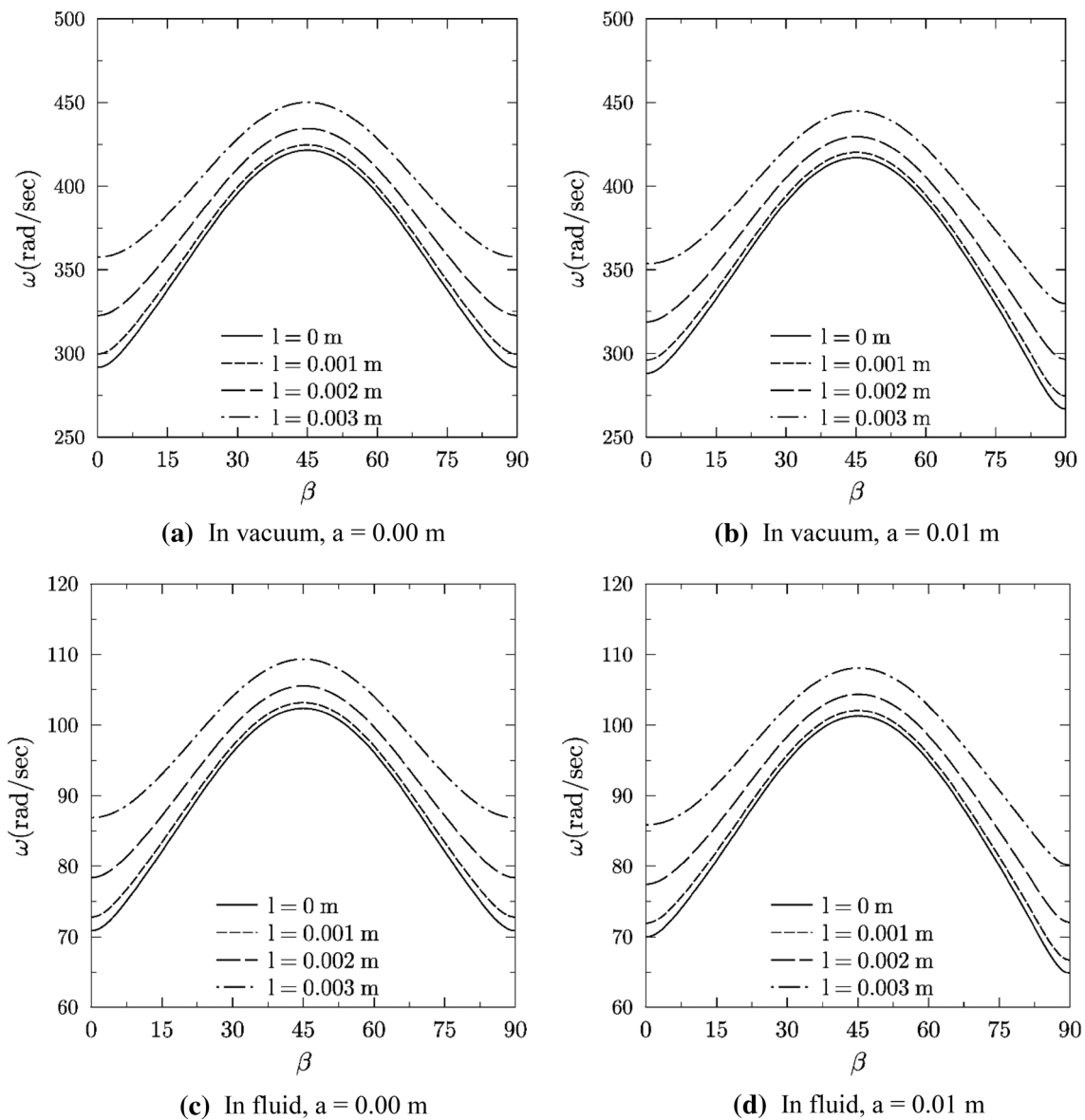
where

Fig. 5 Fundamental frequency (rad/s) for intact and cracked orthotropic plate as affected by material length-scale parameter l (m) for various fibre orientations (β) ($\Delta T = 2$ °C, for in fluid—$h_1/L_1 = 0.1$)

$$I_{11} = \frac{-(D_x + D^{lx})\frac{\pi^4}{L_1^4}\left\{(1+\vartheta_y) - \frac{(\vartheta_y m_y + m_x)}{\frac{1}{G_{xy}} - m_y^2 E_y}(2 - m_y E_y)\right\}}{1 - \frac{E_x(\vartheta_y m_y + m_x)}{(1-\vartheta_x\vartheta_y)\left(\frac{1}{G_{xy}} - m_y^2 E_y\right)}\left(m_x + m_y\vartheta_x\frac{E_y}{E_x}\right)}$$

$$+ \frac{-2\frac{\pi^4}{L_1^4}\left\{\frac{h^3}{6} - \left((D_x + D^{lx})m_x + \vartheta_x(D_y + D^{ly})m_y\right) - \left((D_y + D^{ly})m_y + \vartheta_y(D_x + D^{lx})m_x\right)\right\}}{\frac{1}{G_{xy}} - \frac{m_x E_x(\vartheta_y m_y + m_x) + m_y E_y(\vartheta_x m_x + m_y)}{(1-\vartheta_x\vartheta_y)}}$$

$$+ \frac{-(D_y + D^{ly})\frac{\pi^4}{L_1^4}\left\{(1+\vartheta_x) + \frac{(\vartheta_x m_x + m_y)}{\frac{1}{G_{xy}} - m_x^2 E_x}(-2 + m_x E_x)\right\}}{1 - \frac{E_y(\vartheta_x m_x + m_y)}{(1-\vartheta_x\vartheta_y)\left(\frac{1}{G_{xy}} - m_x^2 E_x\right)}\left(m_y + m_x\vartheta_y\frac{E_x}{E_y}\right)}$$

$$\frac{2a}{3\left(\frac{\alpha_{bt}}{6} + \alpha_{bb}\right)(3+\vartheta_x)(1-\vartheta_x)h + 2a} - \frac{(D_y + D^{ly})\frac{\pi^4}{L_1^4}\left\{(1+\vartheta_x) + \frac{(\vartheta_x m_x + m_y)}{\frac{1}{G_{xy}} - m_x^2 E_x}(-2 + m_x E_x)\right\}}{1 - \frac{E_y(\vartheta_x m_x + m_y)}{(1-\vartheta_x\vartheta_y)\left(\frac{1}{G_{xy}} - m_x^2 E_x\right)}\left(m_y + m_x\vartheta_y\frac{E_x}{E_y}\right)}$$

$$T_{11} = \frac{\pi^2}{L_1^2}\left[\frac{E_x\Delta Th}{1 - \nu_x\nu_y}\left(\frac{(\vartheta_y m_y + m_x)(\alpha_{xy} + m_y E_y\alpha_y)}{\left(\frac{1}{G_{xy}} - m_y^2 E_y\right)} + (\alpha_x + \alpha_y\vartheta_y)\right)\right.$$

$$+ \frac{E_y\Delta Th}{1 - \nu_x\nu_y}\left(1 + \frac{2a}{(6\alpha_{bt} + \alpha_{tt})(1-\vartheta_x^2)h + 2a}\right)\left(\frac{(\vartheta_x m_x + m_y)(\alpha_{xy} + m_x E_x\alpha_x)}{\left(\frac{1}{G_{xy}} - m_x^2 E_x\right)} + (\alpha_x\vartheta_x + \alpha_y)\right)$$

$$\left.-2\left(\frac{\Delta Th(\alpha_{xy} + m_x E_x(\alpha_x + \alpha_y\vartheta_y) + m_y E_y(\alpha_y + \alpha_x\vartheta_x))}{(1 - \vartheta_x\vartheta_y)}\right)\right].$$

The results for central deflection of a cracked orthotropic submerged plate without influence of thermal environment ($\Delta T = 0$), Eq. (39) can be expressed as

$$W_{11}^{\text{cracked}} = \frac{P_{11}}{I_{11} - C_{11} - (\rho h + m_{\text{add}})\emptyset^2}. \tag{40}$$

Similarly, the result for central deflection of a uniformly heated intact orthotropic submerged plate without influence of any crack ($a = 0$), Eq. (39) can be expressed as

$$W_{11}^{\text{heated}} = \frac{P_{11}}{I_{11} - T'_{11} - (\rho h + m_{\text{add}})\emptyset^2}, \tag{41}$$

where

$$T'_{11} = \frac{\pi^2}{L_1^2}\left[\frac{E_x\Delta Th}{1 - \nu_x\nu_y}\left(\frac{(\vartheta_y m_y + m_x)(\alpha_{xy} + m_y E_y\alpha_y)}{\left(\frac{1}{G_{xy}} - m_y^2 E_y\right)} + (\alpha_x + \alpha_y\vartheta_y)\right)\right.$$

$$+ \frac{E_y\Delta Th}{1 - \nu_x\nu_y}\left(\frac{(\vartheta_x m_x + m_y)(\alpha_{xy} + m_x E_x\alpha_x)}{\left(\frac{1}{G_{xy}} - m_x^2 E_x\right)} + (\alpha_x\vartheta_x + \alpha_y)\right)$$

$$\left.-2\left(\frac{\Delta Th(\alpha_{xy} + m_x E_x(\alpha_x + \alpha_y\vartheta_y) + m_y E_y(\alpha_y + \alpha_x\vartheta_x))}{(1 - \vartheta_x\vartheta_y)}\right)\right].$$

The result for central deflection of an intact orthotropic submerged plate without influence of any crack ($a = 0$), thermal environment ($\Delta T = 0$) and fibre orientation ($\beta = 0°$), Eq. (39), can be expressed as

$$W_{11}^{\text{intact}} = \frac{P_{11}}{\frac{\pi^4}{L_1^4}(D_x + 2B + D_y) - \emptyset^2(\rho h + m_{\text{add}})}. \tag{42}$$
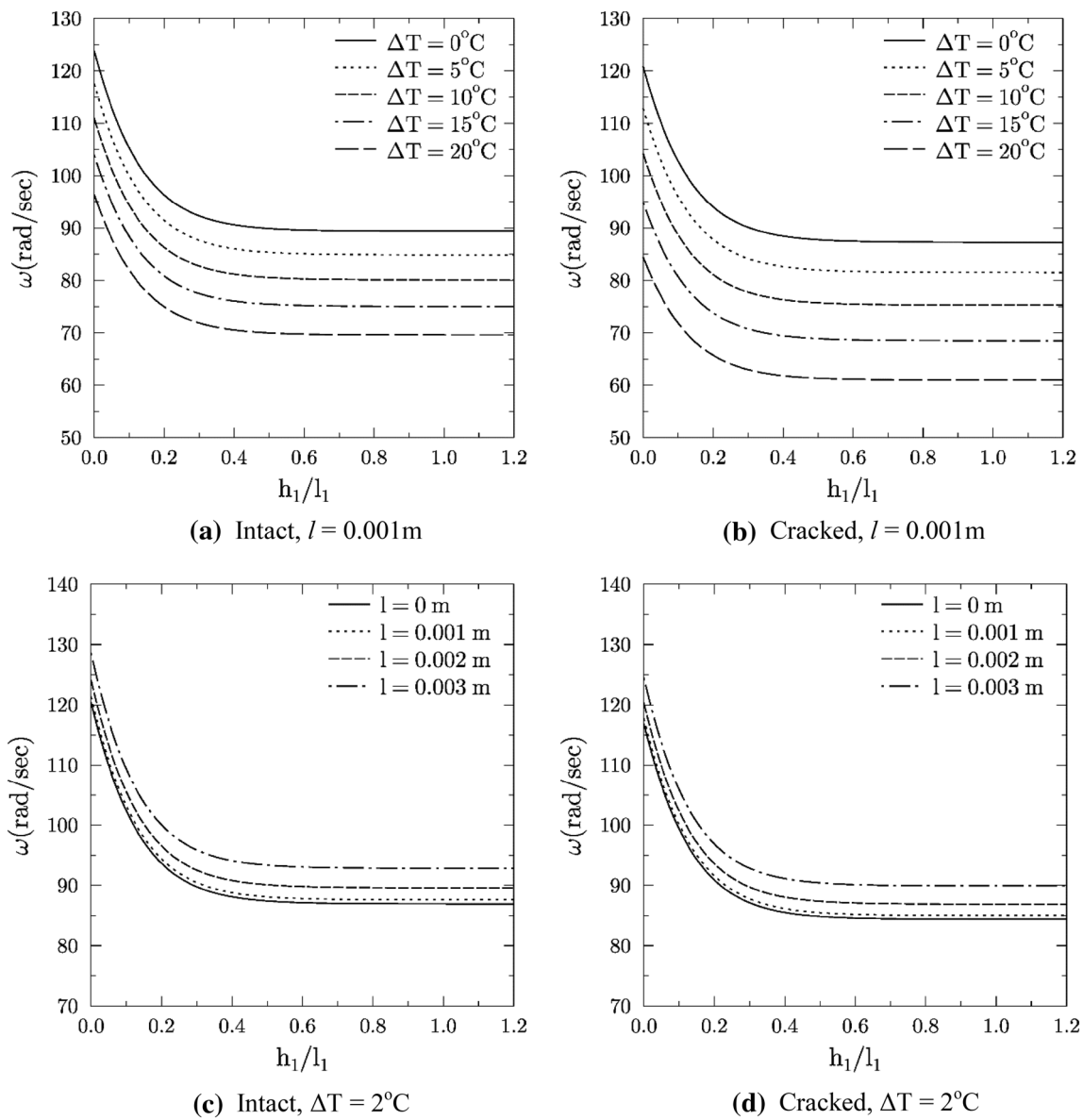
Fig. 6 Fundamental Frequency (rad/s) of an intact and cracked orthotropic submerged plate as affected by temperature (ΔT) and internal length-scale parameter (l) for different level of submergence ($\beta = 45°$, for cracked—$a = 0.05$ m)

The central deflection ratio $W_{11}^{\text{cracked}} / W_{11}^{\text{intact}}$ can be obtained by dividing Eqs. (40) and (42) as

$$\frac{W_{11}^{\text{cracked}}}{W_{11}^{\text{intact}}} = \frac{\frac{\pi^4}{L_1^4}\left(D_x + 2B + D_y\right) - \left(\rho h + m_{\text{add}}\right)\emptyset^2}{I_{11} - C_{11} - \left(\rho h + m_{\text{add}}\right)\emptyset^2} \tag{43}$$

or

$$\frac{W_{11}^{\text{cracked}}}{W_{11}^{\text{intact}}} = \frac{\left(\emptyset/\omega\right)^2}{\frac{L_1^4\left(I_{11} - C_{11}\right)}{\pi^4\left(D_x + 2B + D_y\right)} - \left(\emptyset/\omega\right)^2}, \tag{44}$$

where $\omega = \sqrt{\frac{\frac{\pi^4}{L_1^4}\left(D_x + 2B + D_y\right)}{\left(\rho h + m_{\text{add}}\right)}}$ is the natural frequency of intact orthotropic submerged plate.

Similarly, the central deflection ratio $W_{11}^{\text{heated}} / W_{11}^{\text{intact}}$ can be obtained by dividing Eqs. (41) and (42) as

$$\frac{W_{11}^{\text{heated}}}{W_{11}^{\text{intact}}} = \frac{1 - \left(\emptyset/\omega\right)^2}{\frac{L_1^4\left(I_{11} - T_{11}'\right)}{\pi^4\left(D_x + 2B + D_y\right)} - \left(\emptyset/\omega\right)^2}. \tag{45}$$

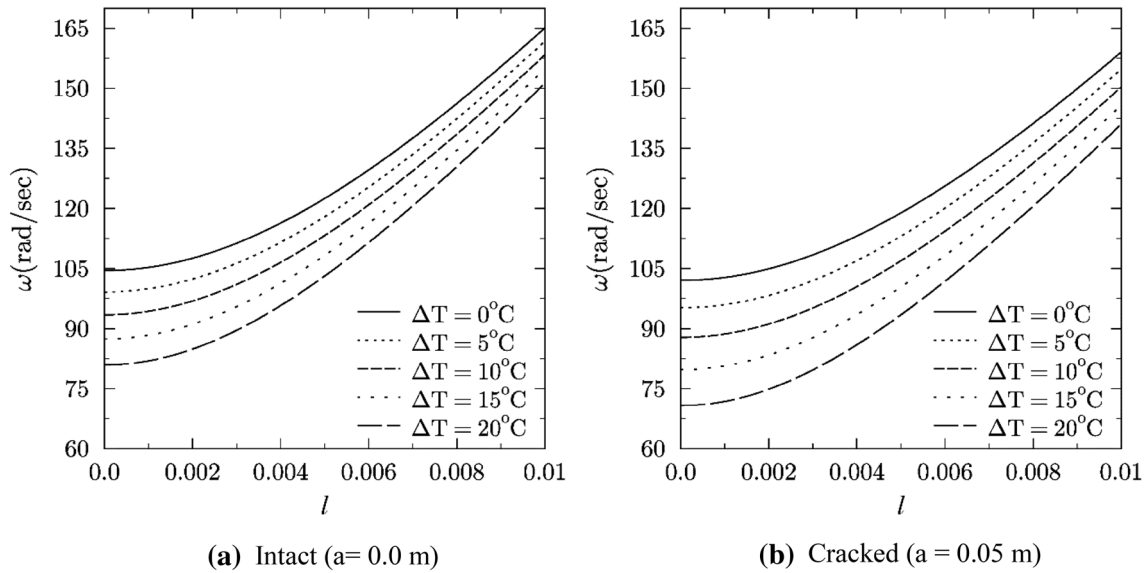**(a)** Intact (a= 0.0 m)   **(b)** Cracked (a = 0.05 m)

Fig. 7 Fundamental frequency (rad/s) of orthotropic submerged plate as affected by temperature (ΔT) and internal length-scale parameter l (m) ($\beta = 45°$, $h_1/L_1 = 0.1$)

Table 3 Fundamental frequency for a cracked orthotropic plate as affected by crack location and temperature variation for different fibre orientation in vacuum ($a = 0.2$ m, $l = 0.001$ m)

Fundamental frequency (ω_{mn})

ξ_c	Fibre angle (β)	Rise in temperature (ΔT)			
		$\Delta T = 0$ °C	$\Delta T = 1$ °C	$\Delta T = 2$ °C	$\Delta T = 3$ °C
0	0	322.169	303.961	284.590	263.801
	15	346.129	335.631	324.794	313.582
	30	397.537	390.086	382.491	374.742
	45	420.856	415.067	409.196	403.239
	60	394.492	387.815	381.021	374.104
	75	328.542	317.578	306.222	294.428
	90	238.362	206.110	167.768	117.519
0.1	0	324.451	306.938	288.363	268.507
	15	348.555	338.704	328.559	318.090
	30	399.758	392.821	385.759	378.565
	45	423.283	417.855	412.355	406.782
	60	397.918	391.626	385.230	378.726
	75	336.193	326.144	315.775	305.054
	90	265.194	239.062	209.698	175.488
0.2	0	325.217	307.924	289.600	270.036
	15	349.439	339.806	329.892	319.670
	30	400.582	393.819	386.939	379.933
	45	424.160	418.852	413.477	408.030
	60	399.101	392.931	386.663	380.292
	75	338.695	328.927	318.860	308.464
	90	273.366	248.826	221.585	190.488

Table 4 Fundamental frequency for a cracked orthotropic submerged plate as affected by crack location and temperature variation for different fibre orientation ($a = 0.2$ m, $l = 0.001$ m, $h_1/l_1 = 0.1$)

Fundamental frequency (ω_{mn})

ξ_c	Fibre angle (β)	Rise in temperature (ΔT)			
		$\Delta T = 0$ °C	$\Delta T = 1$ °C	$\Delta T = 2$ °C	$\Delta T = 3$ °C
0	0	78.255	73.832	69.127	64.077
	15	84.075	81.525	78.892	76.169
	30	96.562	94.752	92.907	91.025
	45	102.226	100.820	99.394	97.947
	60	95.822	94.200	92.550	90.870
	75	79.803	77.140	74.381	71.517
	90	57.898	50.064	40.751	28.545
0.1	0	78.809	74.555	70.044	65.220
	15	84.664	82.271	79.807	77.264
	30	97.101	95.416	93.701	91.954
	45	102.815	101.497	100.161	98.807
	60	96.654	95.126	93.572	91.993
	75	81.661	79.220	76.702	74.098
	90	64.416	58.068	50.936	42.626
0.2	0	78.995	74.795	70.344	65.592
	15	84.879	82.539	80.131	77.648
	30	97.301	95.659	93.987	92.286
	45	103.029	101.739	100.434	99.111
	60	96.942	95.443	93.921	92.373
	75	82.269	79.896	77.451	74.926
	90	66.401	60.440	53.823	46.269

Results and Discussion

In this section, new results for fundamental frequency and central deflection of a cracked orthotropic submerged plate as affected by crack length (a), crack location (ξ_c), fibre orientation (β), level of submergence (h_1/L_1), rise in temperature (ΔT) and microstructure (l) are presented for SSSS boundary condition. The orthotropic plate under consideration is made up of Boron Epoxy; the material properties are considered same as that used in Refs. [10, 56]: $E_x = 208 \times 10^9$ Pa, $E_y = 18.9 \times 10^9$ Pa, $\vartheta_1 = 0.23$, $\vartheta_2 = 0.0208$, $G_{12} = 5.7 \times 10^9$ Pa and $\rho = 2000$ kg/m^3. The coefficients of thermal expansion taken are $\alpha_x = 7.10\mathrm{e}-06/°\mathrm{C}$ and $\alpha_y = 2.3\mathrm{e}-05/°\mathrm{C}$. The fluid density is 1000 kg m^{-3}. The dimensions of reservoir tank are 5 m × 5 m × 5 m. The depth of crack is 0.006 m and the plate thickness is 0.01 m throughout this work. The plate dimensions are taken as $L_1 = L_2 = 1$ m. As the literature lacks in the results for orthotropic submerged plate, validation of the present model is done with the cracked orthotropic plate in vacuum medium. Table 1 represents the results for frequency parameter of an intact and cracked orthotropic plate for various fibre orientations and length-scale parameters. The material constants of plate for this validation (Table 1) are taken from Ref. [56]. Results in Table 1 shows that the present outcomes are in exact agreement with the existing results which verifies the correctness of the proposed model.

To compare the effect of level of submergence (fluidic medium), the present model is applied for a partially cracked isotropic submerged plate and the compared results for fundamental frequency parameter are shown in Table 2. The material constants and plate dimensions for results in Table 2 are taken from Ref. [11]. Again, the results are in exact agreement with the existing results which indicates that the proposed model deduces to the model developed by Ref. [11] when applied for an isotropic plate. In the absence of fluidic medium, the results for fundamental frequency of especially orthotropic cracked plate as affected by thermal environment can be found in the literature (Ref. [10]). The present model reduces to the one presented by Ref [10] when applied for a cracked orthotropic plate in the absence of fluidic medium with fibre orientation at 0° and 90°. Therefore, such validation is omitted here.

Figure 4 shows new results for the variation in fundamental frequency of intact and cracked orthotropic plates with fibre orientations ($\beta = 0$–90°) and temperature ($\Delta T = 0$–8 °C) for two different surrounding mediums (vacuum and fluid). It is well known that, for a square intact orthotropic plate, the fundamental frequency increases gradually from fibre orientation 0° to 45° (maximum) and is symmetric for 45°–90°. A similar trend is seen in the present results for an intact orthotropic plate (Fig. 4a, c), for both the surrounding
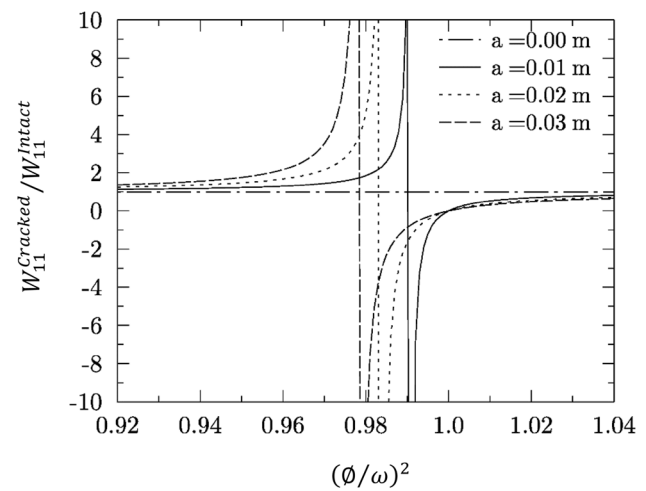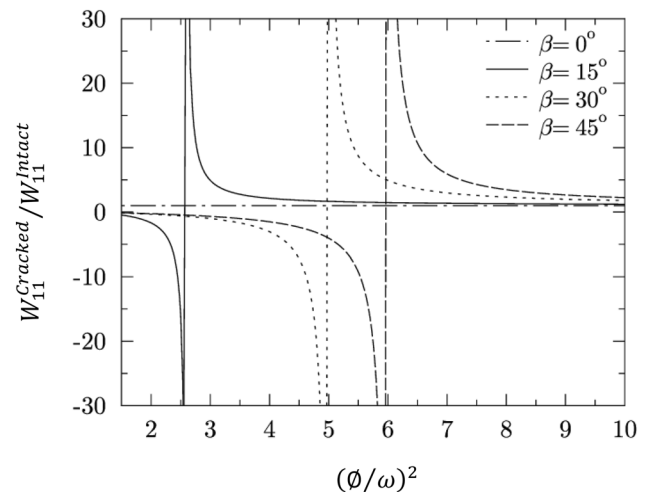

Fig. 8 Central deflection ratio $W_{11}^{\text{cracked}}/W_{11}^{\text{intact}}$ versus the normalized operational frequency $(\emptyset/\omega)^2$ for various values of crack length (a) in metres. ($\Delta T = 0$, $\beta = 0°$, $l = 0$ m)

Fig. 9 Central deflection ratio $W_{11}^{\text{cracked}}/W_{11}^{\text{intact}}$ versus the normalized operational frequency $(\emptyset/\omega)^2$ for various values of fibres angle ($\beta°$) ($\Delta T = 0$, $a = 0.01$ m, $l = 0$ m)

mediums when the fibres are oriented from 0° to 90°. But in case of the cracked plate (Fig. 4b, d), it is observed that, due to presence of crack, the pattern of frequency variation for various fibre orientations is not symmetrical about 45°. This is because the crack under consideration is parallel to either edges of the plate and for every fibre orientation the stiffness is differently affected. In Fig. 4b, d it is clearly seen that stiffness is least affected when fibres are at 0° and most when fibres are at 90°, i.e. crack is across the fibres which satisfies one's physical understanding. Literature shows that the rise in temperature of cracked isotropic plate reduces its frequency (Ref. [9]). Such a reduction in frequency is due to decrease in stiffness which is also observed to be
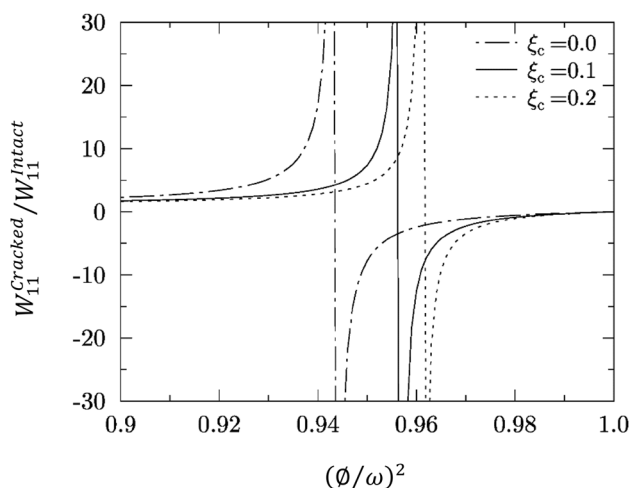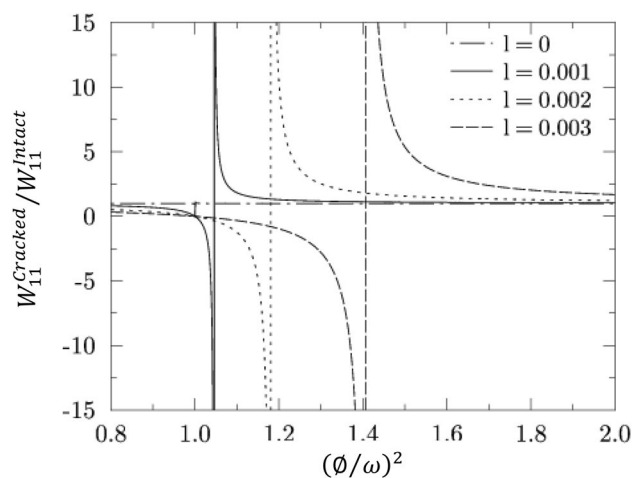
Fig. 10 Central deflection ratio $W_{11}^{cracked}/W_{11}^{intact}$ versus the normalized operational frequency $(\emptyset/\omega)^2$ for various values of crack location (ξ_c) ($a = 0.2$ m, $\Delta T = 0$, $\beta = 0°$, $l = 0$ m)
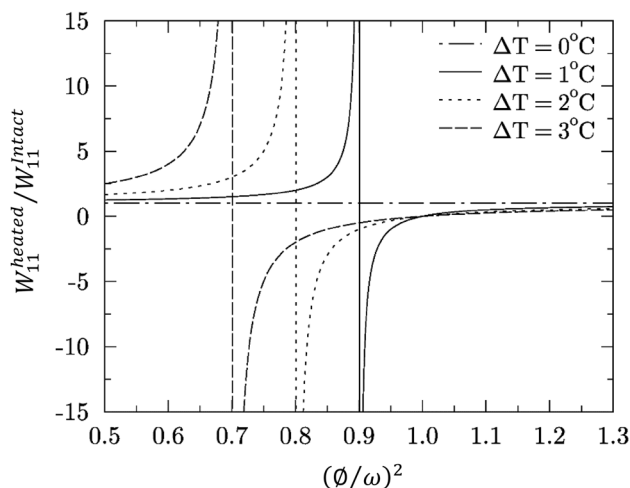

Fig. 12 Central deflection ratio $W_{11}^{cracked}/W_{11}^{intact}$ versus the normalized operational frequency $(\emptyset/\omega)^2$ for various values of internal material length-scale parameter (l) in metres. ($\Delta T = 0$, $a = 0.01$ m, $\beta = 0°$, $z = 0$ m)

Fig. 11 Central deflection ratio $W_{11}^{heated}/W_{11}^{intact}$ versus the normalized operational frequency $(\emptyset/\omega)^2$ for various values of temperature ΔT. ($a = 0$ m, $\beta = 0°$, $l = 0$ m)

valid for cracked orthotropic plate in both the vacuum and fluid medium in present case. It is interesting to see from Fig. 4a–d that with every fibre orientation, the reduction in frequency with uniform rise in temperature ($\Delta T = 0$–8 °C) is different. It is noted that the reduction in frequency at 45° of fibre orientation is less when compared to 0° and 90° for both intact and cracked orthotropic plates, it is due to the thermal stresses induced for a given temperature at 45° fibre orientation is less as compared to 0 and 90° and hence the reduction in the stiffness due to temperature is lesser at 45°.

Again it is also observed from Fig. 4a, b (in vacuum) and Fig. 4c, d (in fluid) that the frequencies are reduced in fluidic medium as compared to plate in vacuum. This is

because of the virtual added mass (m_{add}) due to surrounding fluid which increases the overall mass (M_{mn}) of coupled system as shown in Eq. (33), thus validating one's physical understanding. Similar type of variation in frequencies due to fluidic medium is also evident in the works of Ref. [11] for isotropic plates thereby validating the present variations for orthotropic plate.

By employing the modified couple stress theory, the variation in fundamental frequency of an intact and cracked orthotropic plate with internal length-scale parameter (l) is shown in Fig. 5. It is seen that for a given fibre orientation angle as the material length-scale parameter increases ($l = 0$–0.003 m) the fundamental frequency also increases, such increase in frequency is due to the contribution of microstructure to the flexural rigidity of the plate. It can be noted that classical plate theory under-predicts the frequency in the case of a micro-plate and the difference in both the theories is noticeable. Figure 5c, d shows such variation is observed to be valid for the case of intact and cracked orthotropic submerged plates also. Therefore, the consideration of microstructure in terms of material length-scale parameter is significant. It is important to mention that the frequency decreases due to the presence of crack whereas it increases when the internal length-scale parameter is considered. From Figs. 4 and 5 it is found that the effect of variation in temperature and length-scale parameter on fundamental frequency for a given fibre orientation is same for submerged plate as well as plate in vacuum. Such similarity is due to the assumption that the rise in temperature and length-scale parameter does not affect the virtual added mass (m_{add}).

The comparison of variation in fundamental frequency as affected by temperature and internal length-scale parameter for various level of submergence is shown in Fig. 6

for a fixed fibre orientation ($\beta = 45°$). It is observed from Fig. 6a–d that for a given temperature difference and length-scale parameter, as the plate goes deeper into the fluid tank, i.e. with the increase in depth of submergence, the frequency of the plate decreases for both intact and cracked plates. This is due to the resistance offered by the fluid medium in the form of dynamic pressure to the vibratory motion of plate. As the submerged plate goes deep into the fluid, the mass of fluid layer vibrating with the plate increases thereby increasing the virtual added mass or the total mass of the coupled system. Such a phenomenon of variation in frequency is also found in Refs. [20, 11] for intact and cracked isotropic plates, respectively. It is seen from Fig. 6a, b that for a given level of submergence, as the temperature of plate is increased from $\Delta T = 0$–20 °C, the frequency is decreased, which is again due to the decrease in the thermal stiffness of the plate which further reduces the overall plate's stiffness. It is interesting to see from Fig. 6b that for the cracked plate at a fixed level of submergence, the reduction in frequency as affected by temperature variation is found to be more when compared to intact plate (Fig. 6a). The reason behind such reduction in frequency is for an intact plate, decrease in stiffness is only due to thermal stress but for a cracked plate, it is due to thermal stresses as well as due to effect of crack. This interaction between the crack and temperature is clearly shown by the third term in the expression for plate's stiffness [Eq. (34)]. Thus, it is concluded that the presence of thermal environment and crack in an orthotropic plate can severely affect the fundamental frequency of plate. Again, it is seen from Fig. 6c, d that for a given level of submergence as the internal length-scale parameter increases ($l = 0$–0.003 m), the fundamental frequency also increases due to the effect of microstructure.

From Fig. 7a, b, it is observed that for a given length-scale parameter, the fundamental frequency decreases with the increase in temperature ($\Delta T = 0$–20 °C). It is found that for higher values of length-scale parameter ($l = 0.01$), the effect of increase in temperature on frequency reduces; this is because of the substantial contribution of material length-scale parameter to the stiffness.

Tables 3 and 4 show the results for fundamental frequency as a function of crack location and temperature variation for cracked plate vibrating in vacuum and fluid, respectively. Plate dimension considered are $L_1 = L_2 = 1$ m for both the tables and all the results are obtained for SSSS boundary condition. The crack length is kept constant at $a = 0.2$ m and internal material length-scale parameter at $l = 0.001$ m. It is seen from both the tables that as the crack moves away from the centre the fundamental frequency increases, this is because the crack at centre of the plate affects the stiffness to maximum as compare to other locations. A similar phenomenon was seen in Ref. [56] in the absence of thermal environment. Thus, it can be concluded that for the case of

thermal environment also, the crack at the centre affects the fundamental frequency more when compared to crack at any other location. Again, it is seen that the crack location affects the stiffness most for the fibre orientation 90° (crack across the fibres) and least for 0° (crack parallel to the fibres). It is because the crack is parallel to either edges of the plate and with every orientation of fibre plate's stiffness is differently affected. From Tables 3 and 4, it is also found that the effect of crack locations on fundamental frequency for a given temperature and fibre orientation is same for submerged plate and plate in vacuum. This is due to the assumption that the crack terms do not affect the virtual added mass (m_{add}) of plate.

Figure 7 represents the variation of ratio of deflection of cracked plate to intact orthotropic plate. To investigate the primary resonance, the ratio of forcing frequency to fundamental frequency of intact plate based on strain gradient theory is varied from 0.92 to 1.04. It is interesting to note that the presence of crack shifts the primary resonance and it takes place well below $\emptyset/\omega = 1$. This is due to the reduction in plate's stiffness due to centrally located crack. Similarly, the effect of fibre orientation and crack location on deflection of cracked plate is shown in Figs. 9 and 10, respectively. The results for variation of deflection ratio of heated intact plate to intact plate with respect to the ratio of forcing frequency and fundamental frequency are shown in Fig. 11. With the rise in temperature of plate, it is known that the fundamental frequencies decrease; such a fact seen in the literature is validated from the results of Fig. 11. As expected, the rise of temperature decreases the fundamental frequency of plate thereby increasing the deflection. The shift in primary resonance can be ascribed to the decrease in plate's stiffness due to temperature rise. Figure 12 shows the ratio of deflections $W_{11}^{\text{cracked}}/W_{11}^{\text{intact}}$ versus $(\emptyset/\omega)^2$ for various values of length scale of microstructure (l). It is seen that increasing values of l result in shifting the primary resonance position of the classical case ($\emptyset/\omega = 1$) to higher values of ($\emptyset/\omega$). The shift in primary resonance can be attributed to the increase in stiffness due to internal length scale of microstructure. Thus, it can be concluded that the primary resonance occurs at higher values of forcing frequency ($\emptyset$). As per the authors' knowledge, Figs. 8, 9, 10, 11 and 12 along with Eqs. (38–45) present first time the effect of crack length, crack location, fibre orientation, temperature and length scale of microstructure on deflection and primary resonance of cracked orthotropic submerged plate.

Conclusions

Micro-sized structures such as micro-plate have recently emerged as promising frequency sensing devices. In practice, these micro-plates are often operated under different

surroundings such as fluidic medium and thermal environment. For, e.g. a micro-plate when used as a bio-sensor needs to interact with biological particles in natural fluid–thermal environment. When these micro-plates are used as frequency sensing devices, they usually undergo dynamic loading and when submerged in fluidic medium they also bear fluid inertial loads. Due to such dynamic loading, micro-plates are prone to develop flaws such as cracks, this is in line with one's physical understanding and hence, it is necessary to predetermine its characteristics at the design level.

To cater the above problem, on the basis of classical plate theory and modified couple stress theory, vibration and deflection analyses of submerged orthotropic micro-plate with arbitrarily located crack are investigated in the presence of thermal environment. For this purpose, the governing differential equation is derived following the equilibrium principle and analytically solved for the simply supported boundary condition. A classical relation for central deflection of cracked plate affected by forcing frequency, crack length and its location, temperature, material length-scale parameter and fibre environment is also deduced in the present work.

The effects of crack length, crack location, fibre orientation, level of submergence, material length-scale parameter and thermal environment are examined in detail for boron-epoxy orthotropic micro-plate. It is established that the fundamental frequency of plate decreases by the presence of crack and thermal environment and this decrease in frequency is further intensified by presence of surrounding fluid medium in the present study. It is further observed that the presence of centrally located crack affects the frequency differently for each fibre orientation. It is because the crack is assumed to be parallel to either edge of the plate and with every orientation of fibre plate's stiffness is differently affected. Another important conclusion is that with the increase in temperature variation the reduction in frequency at 45° of fibre orientation is less as compared to 0 and 90° for both intact and cracked orthotropic plate. It is known from the strength point of view that 45° fibre orientation makes the plate stronger and the present work proves this to be true for orthotropic micro-plate in the presence of partial crack, fluid and thermal environment. Few results are presented in tabular and graphical form to show the comparative differences between the results obtained by classical plate theory and modified couple stress theory.

The rise in temperature and increase in crack length shifts the resonance to lower values of forcing frequency whereas the increase in fibre orientation and length-scale parameter shift the resonance to higher values. It is also seen that as the crack moves away from centre the resonance also shifts to higher values of forcing frequency, this is because the crack at centre of plate affects the frequency to maximum as compared to other locations.

Compliance with Ethical Standards

Appendix A

From the literature review, it is seen that many researchers used strain gradient (higher order) theories [38, 40, 46, 65–67] to consider the size effect of microstructure in form of length-scale parameter. Among them Tsiatas [43] and Yin et al. [46] proposed a new non-classical Kirchhoff's plate model with a single internal material length-scale parameter for the analysis of isotropic micro-plates based on the simplified couple stress theory of Yang et al. [67].

In the simplified couple stress theory, the strain energy density (U) in three-dimensional body occupying a volume V bounded by the surface G is given by Yang et al. [67] as

$$U = \frac{1}{2} \int \left(\sigma_{ij} \epsilon_{ij} + m_{ij} \aleph_{ij} \right) \mathrm{d}V, \tag{46}$$

where

$$\epsilon_{ij} = \frac{1}{2} \left(\frac{\partial u_i}{\partial j} + \frac{\partial u_j}{\partial i} \right), \tag{47}$$

$$\aleph_{ij} = \frac{1}{2} \left(\frac{\partial \theta_i}{\partial j} + \frac{\partial \theta_j}{\partial i} \right), \tag{48}$$

are the strain tensor (ϵ_{ij}) and the symmetric part of the curvature tensor ($\aleph_{ij}$), respectively, u_{ij} is the displacement vector and θ_{ij} is the rotation vector which can defined as

$$\theta_i = \frac{1}{2} e_{ijk} \frac{\partial u_k}{\partial j}, \tag{49}$$

where e_{ijk} is the permutation symbol.

As per modified couple stress theory, the stress tensor (σ_{ij}) and the deviatoric part of the couple stress tensor (m_{ij}) can be expressed as (Ref. [43])

$$\sigma_{ij} = \lambda \epsilon_{kk} \delta_{ij} + 2\mu_o \epsilon_{ij}, \tag{50}$$

$$m_{ij} = 2\mu_o l^2 \aleph_{ij}, \tag{51}$$

where λ and μ_o are the Lamé constants, δ_{ij} is the Kronecker delta. Equations (50) and (51) described the two dimensional state of stress. From Eq. (51) it is observed that the couple stress tensor m_{ij} is symmetric and from Eq. (48) the

curvature tensor $\aleph_{ij}$ is also symmetric. That is, only the symmetric part of the rotation gradient and the symmetric part of displacement gradient contribute to the deformation energy (Ref. [67]) which is dissimilar from that in the classical couple stress theory.

In the work of Tsiatas [43], after the suitable replacement of the Lamé constants by the modulus of elasticity E and the Poisson's ratio v, the stress tensor (σ_{ij}) and the couple stress tensor (m_{ij}) is expressed as

$$\sigma_{\alpha\beta} = \frac{E}{1-v^2}\left[v\epsilon_{kk}\delta_{\alpha\beta} + (1-v)\epsilon_{\alpha\beta}\right], \tag{52}$$

$$m_{\alpha\beta} = 2Gl^2\aleph_{\alpha\beta}, \tag{53}$$

where $G = E/2(1+v)$ is the shear modulus, l is a material length-scale parameter and $\aleph_{ij}$ is the curvature tensor.

From Eqs. (52) and (53), the expression for the bending moment and couple moment tensors can be written as [43]

$$M_{\alpha\beta} = \int_{-\frac{h}{2}}^{\frac{h}{2}} \sigma_{\alpha\beta} z\mathrm{d}z, \tag{54}$$

$$Y_{\alpha\beta} = \int_{-\frac{h}{2}}^{\frac{h}{2}} m_{\alpha\beta}\mathrm{d}z. \tag{55}$$

Expressing the curvature and strain tensors in form of lateral deflection of isotropic plate we have (Ref. [43])

$$M_x = M_{11} = -D\left(\frac{\partial^2 w}{\partial x^2} + v\frac{\partial^2 w}{\partial y^2}\right) \quad Y_x = Y_{11} = 2D^l\frac{\partial^2 w}{\partial x\partial y},$$

$$M_y = M_{22} = -D\left(\frac{\partial^2 w}{\partial y^2} + v\frac{\partial^2 w}{\partial x^2}\right) \quad Y_y = Y_{22} = -2D^l\frac{\partial^2 w}{\partial x\partial y},$$

$$M_{xy} = M_{11} = M_{yx} = M_{22} = D(1-v)\frac{\partial^2 w}{\partial x\partial y}$$

$$Y_{xy} = Y_{yx} = Y_{12} = Y_{21} = D^l\left(\frac{\partial^2 w}{\partial y^2} - \frac{\partial^2 w}{\partial x^2}\right),$$

where $D = \frac{Eh^3}{12(1-v^2)}$ is the flexural rigidity of the isotropic plate and $D^l = \frac{El^2h}{2(1+v)}$ shows the bending rigidity due to couple stress of micro-plate and l is a material length-scale parameter. This D^l also shows the contribution of rotation gradients to the bending rigidity.

Tsiatas [43] employed the Gauss divergence theorem to the total potential energy of a deformable body and arrived at the expression of bending moment which shows two components of bending; (i) the bending due to microstructure and (ii) pure plate bending. This expression for moment can be written as

$$M_{ii}^* = M_{ii} + M_{ii}^l = -\left(D + D^l\right)\left(\frac{\partial^2 w}{\partial i^2} + v\frac{\partial^2 w}{\partial j^2}\right)$$

$$M_{ij}^* = M_{ij} + M_{ij}^l = \left(D + D^l\right)(1-v)\frac{\partial^2 w}{\partial i\partial j}.$$

From the above expression, it is seen that the effect of microstructure in the form of a single material length-scale parameter "l", contributing to the bending moment and increasing the flexural rigidity by $D^l = \frac{El^2h}{2(1+v)}$. The advantage of the modified couple stress theory developed by Tsiatas [43] is that a single parameter can capture the microstructure effect and its contribution to the flexural rigidity can be easily coupled with the rigidity used in classical plate theory. It is important here to note that Yin et al. [46] employed the additional rigidity (D^l) due to microstructure in their analysis of dynamics of micro-plate. The present work employs the additional flexural rigidity established by Tsiatas [43] for isotropic plate and applies it to the case of cracked orthotropic submerged plate in the presence of thermal environment.

Appendix B

Soni et al. [11] have formulated the fluid forces in form of virtual added mass using potential flow theory and presented the influence of fluid medium on vibration response of cracked isotropic plate. They used the velocity potential function along with Bernoulli's equation to express the fluid dynamic pressures acting on the plate. Similar approach has been adopted here to find the fluid pressure for cracked orthotropic plate with the following assumptions:

1. The fluid flow is assumed to be small, incompressible, homogeneous and irrotational.
2. The dynamic fluid pressure is normal to the surface of the plate and shear forces are neglected as the fluid is inviscid.
3. Interaction between the cracked plate and fluid and influence of non-linearity at plate–fluid interface is neglected.
4. As the orthotropic plate is considered thin, the effect of fluid forces is ignored in the derivation of in-plane forces.
5. The fluid behaves like a thermal reservoir and the rise in temperature does not affect the fluid properties.

The velocity potential function $\phi(x, y, z, t)$ satisfying the Laplace's equation can be expressed in the Cartesian coordinate system as

$$\nabla^2\phi = \frac{\partial^2\phi}{\partial x^2} + \frac{\partial^2\phi}{\partial y^2} + \frac{\partial^2\phi}{\partial z^2} = 0. \tag{56}$$

Using Bernoulli's equation, the fluid dynamic pressure at any point of plate–fluid boundary can be given by

$$P_u = P_{z=0} = -\rho_f\left(\frac{\partial\phi}{\partial t}\right)_{z=0}, \tag{57}$$

$$P_l = P_{z=-h} = -\rho_f\left(\frac{\partial\phi}{\partial t}\right)_{z=-h}, \tag{58}$$

where ρ_f is fluid density per unit volume.

Assuming ϕ be the function of two discrete variables.

$$\phi(x, y, z, t) = F(z)S(x, y, t), \tag{59}$$

where $S(x, y, t)$ and $F(z)$ are the two discrete functions.

For the assumption of permanent contact between the surface of the plate and fluid layer, the kinematic boundary conditions at the fluid–plate interface can be written as (Ref. [11])

$$\left(\frac{\partial\phi}{\partial z}\right)_{z=0} = \frac{\partial w}{\partial t}, \tag{60}$$

$$\left(\frac{\partial\phi}{\partial z}\right)_{z=-h} = \frac{\partial w}{\partial t}. \tag{61}$$

By introducing Eq. (59) in Eqs. (60) and (61) we get

$$S(x, y, t) = \frac{1}{\left(dF(z)/dz\right)_{z=0}}\frac{\partial w}{\partial t}, \tag{62}$$

$$S(x, y, t) = \frac{1}{\left(dF(z)/dz\right)_{z=-h}}\frac{\partial w}{\partial t}. \tag{63}$$

By substituting Eqs. (62) and (63) in Eq. (59) the ϕ on fluid–plate interfaces (i.e. upper and lower surface of plate) can be stated as

$$\phi(x, y, z, t) = \frac{F(z)}{\left(dF(z)/dz\right)_{z=0}}\frac{\partial w}{\partial t}, \tag{64}$$

$$\phi(x, y, z, t) = \frac{F(z)}{\left(dF(z)/dz\right)_{z=-h}}\frac{\partial w}{\partial t}. \tag{65}$$

The following differential equation of second order can be obtained by putting Eq. (64) or (65) into Eq. (56).

$$\frac{d^2F(z)}{dz^2} - \mu^2 F(z) = 0, \tag{66}$$

where μ represents wave number, which can be determined by $\mu = \pi\sqrt{\frac{1}{l_1^2} + \frac{1}{l_2^2}}$ (Ref. [19]).

The general solution for the differential equation (66) can be expressed as

$$F(z) = Ae^{\mu z} + Be^{-\mu z}. \tag{67}$$

On substituting Eq. (67) into Eqs. (64) and (65) we get an expression for ϕ on plate–fluid interface as shown below:

$$\phi(x, y, z, t) = \frac{Ae^{\mu z} + Be^{-\mu z}}{\left(dF(z)/dz\right)_{z=0}}\frac{\partial w}{\partial t}, \tag{68}$$

$$\phi(x, y, z, t) = \frac{Ae^{\mu z} + Be^{-\mu z}}{\left(dF(z)/dz\right)_{z=-h}}\frac{\partial w}{\partial t}, \tag{69}$$

where A and B denote the unknown constants which can be resolved utilizing two extreme limit conditions at plate–fluid interface and at fluid extremity surfaces $z = h_1$ and $z = (h + h_2)$.

Assuming the disturbance because of free surface wave motion of liquid is irrelevant, the accompanying boundary condition can be applied for velocity potential at the free surface of liquid [19]

$$\left(\frac{\partial\phi}{\partial z}\right)_{z=h_1} = -\frac{1}{g_a}\left(\frac{\partial^2\phi}{\partial t^2}\right)_{z=h_1}, \tag{70}$$

where 'g_a' denotes the gravity acceleration. Substitution of Eq. (68) into Eqs. (70) and (60) gives the expression for velocity potential ϕ as

$$\phi(x, y, z, t) = \frac{1}{\mu}\left[\frac{e^{\mu z} + Ce^{-\mu(z-2h_1)}}{1 - Ce^{2\mu h_1}}\right]\frac{\partial w}{\partial t}, \tag{71}$$

where $C = \frac{g_a\mu - \omega^2}{g_a\mu - \omega^2}$ and ω represents wave motion frequency at free surface of fluid.

The fluid pressure acting on plate's upper surface can be obtained by substituting Eq. (71) of velocity potential into Eq. (57) as

$$P_u = -\frac{\rho_f}{\mu}\left[\frac{1 + Ce^{2\mu h_1}}{1 - Ce^{2\mu h_1}}\right]\frac{\partial^2 w}{\partial t^2}. \tag{72}$$

The boundary condition at the rigid base of the tank represented in Fig. 1 is referred to null-frequency condition and can be written as

$$\left(\frac{\partial \phi}{\partial z}\right)_{z=-\left(h+h_2\right)} = 0. \tag{73}$$

On substituting Eq. (69) into Eqs. (73) and (61), the expression for ϕ is obtained as

$$\phi(x,y,z,t) = \frac{1}{\mu}\left[\frac{e^{\mu z} + e^{-2\mu(h+h_2)}e^{-\mu z}}{e^{-\mu h} - e^{-2\mu(h+h_2)}e^{\mu h}}\right]\frac{\partial w}{\partial t}. \tag{74}$$

From Eqs. (74) and (58), the fluid pressure at plate's lower surface can be expressed as

$$P_l = -\frac{\rho_f}{\mu}\left[\frac{1 + e^{-2\mu h_2}}{1 - e^{-2\mu h_2}}\right]\frac{\partial^2 w}{\partial t^2}. \tag{75}$$

The resulting fluid dynamic pressure for the plate fully submerged in fluid is written as

$$\Delta P = P_u - P_l = -\frac{\rho_f}{\mu}\left[\frac{1 + Ce^{2\mu h_1}}{1 - Ce^{2\mu h_1}} - \frac{1 + e^{-2\mu h_2}}{1 - e^{-2\mu h_2}}\right]\frac{\partial^2 w}{\partial t^2}, \tag{76}$$

$$\Delta P = m_{add}\frac{\partial^2 w}{\partial t^2}, \tag{77}$$

where $m_{add} = -\frac{\rho_f}{\mu}\left[\frac{1+Ce^{2\mu h_1}}{1-Ce^{2\mu h_1}} - \frac{1+e^{-2\mu h_2}}{1-e^{-2\mu h_2}}\right]$ represents the virtual added mass of submerged plate.

References

1. Rice J, Levy N (1972) The part-through surface crack in an elastic plate. J Appl Mech 1:185–194. https://doi.org/10.1115/1.3422609
2. King RB (1983) Elastic-plastic analysis of surface flaws using a simplified line-spring model. Eng Fract Mech 18:217–231. https://doi.org/10.1016/0013-7944(83)90108-X
3. Zhao-jing zeng Z, Shu-ho D (1994) Stress intensity factors for an inclined surface crack under biaxial. Eng Fract Mech 47:281–289
4. Solecki R (1983) Bending vibration of a simply supported rectangular plate with a crack parallel to one edge. Eng Fract Mech 18:1111–1118. https://doi.org/10.1016/0013-7944(83)90004-8
5. Liew KM, Hung KC, Lim MK (1994) A solution method for analysis of cracked plates under vibration. Eng Fract Mech 48:393–404. https://doi.org/10.1016/0013-7944(94)90130-9
6. Malhotra SK, Ganesan N, Veluswami MA (1988) Effect of fibre orientation and boundary conditions on the vibration behaviour of orthotropic square plates. Compos Struct 9:247–255. https://doi.org/10.1016/S0022-460X(88)80377-8
7. Israr A, Cartmell MP, Manoach E, Trendafilova I, Ostachowicz W, Krawczuk M et al (2009) Analytical modelling and vibration analysis of cracked rectangular plates with different loading and boundary conditions. J Appl Mech 76:1–9. https://doi.org/10.1115/1.2998755
8. Ismail R, Cartmell MP (2012) An investigation into the vibration analysis of a plate with a surface crack of variable angular orientation. J Sound Vib 331:2929–2948. https://doi.org/10.1016/j.jsv.2012.02.011
9. Joshi PV, Jain NK, Ramtekkar GD (2015) Effect of thermal environment on free vibration of cracked rectangular plate: an analytical approach. Thin-Walled Struct 91:38–49. https://doi.org/10.1016/j.tws.2015.02.004
10. Joshi PV, Jain NK, Ramtekkar GD, Singh Virdi G (2016) Vibration and buckling analysis of partially cracked thin orthotropic rectangular plates in thermal environment. Thin-Walled Struct 109:143–158. https://doi.org/10.1016/j.tws.2016.09.020
11. Soni S, Jain NK, Joshi PV (2018) Vibration analysis of partially cracked plate submerged in fluid. J Sound Vib 412:28–57. https://doi.org/10.1016/j.jsv.2017.09.016
12. Soni S, Jain NK, Joshi PV (2017) Analytical modeling for nonlinear vibration analysis of partially cracked thin magneto-electro-elastic plate coupled with fluid. Nonlinear Dyn 90(1):137–170. https://doi.org/10.1007/s11071-017-3652-5
13. Lai SK, Zhang LH (2018) Thermal effect on vibration and buckling analysis of thin isotropic/orthotropic rectangular plates with crack defects. Eng Struct 177:444–458. https://doi.org/10.1016/j.engstruct.2018.07.010
14. Lamb H (1920) On the vibrations of an elastic plate in contact with water. Proc Royal Soc Lond Ser A 98:205–216. http://www.jstor.org/stable/93996 Accessed 2016
15. Muthuveerappan G, Ganesan N, Veluswami MA (1979) A note on vibration of a cantilever plate immersed. J Sound Vib 63(3):385–391
16. Kwak MK (1996) Hydroelastic vibration of rectangular plates. J Appl Mech 63:110. https://doi.org/10.1115/1.2787184
17. Amabili M, Frosali G, Kwak MK (1996) Free vibrations of annular plates coupled with fluids. J Sound Vib 191:825–846. https://doi.org/10.1006/jsvi.1996.0158
18. Haddara MR, Cao S (1996) A study of the dynamic response of submerged rectangular flat plates. Mar Struct 9:913–933. https://doi.org/10.1016/0951-8339(96)00006-8
19. Kerboua Y, Lakis AA, Thomas M, Marcouiller L (2008) Vibration analysis of rectangular plates coupled with fluid. Appl Math Model 32:2570–2586. https://doi.org/10.1016/j.apm.2007.09.004
20. Hosseini-Hashemi S, Karimi M, Rokni H (2012) Natural frequencies of rectangular Mindlin plates coupled with stationary fluid. Appl Math Model 36:764–778. https://doi.org/10.1016/j.apm.2011.07.007
21. Liu T, Wang K, Dong QW, Liu MS (2009) Hydroelastic natural vibrations of perforated plates with cracks. Procedia Eng 1:129–133. https://doi.org/10.1016/j.proeng.2009.06.030
22. Si XH, Lu WX, Chu FL (2012) Modal analysis of circular plates with radial side cracks and in contact with water on one side based on the Rayleigh–Ritz method. J Sound Vib 331:231–251. https://doi.org/10.1016/j.jsv.2011.08.026
23. Si X, Lu W, Chu F (2012) Dynamic analysis of rectangular plates with a single side crack and in contact with water on one side based on the Rayleigh–Ritz method. J Fluids Struct 34:90–104. https://doi.org/10.1016/j.jfluidstructs.2012.06.005
24. Yang J, Shen HS (2002) Vibration characteristics and transient response of shear-deformable functionally graded plates in thermal environments. J Sound Vib 255:579–602. https://doi.org/10.1006/jsvi.2001.4161
25. Jeyaraj P, Padmanabhan C, Ganesan N (2008) Vibration and acoustic response of an isotropic plate in a thermal environment. J Vib Acoust 130:51005. https://doi.org/10.1115/1.2948387
26. Jeyaraj P, Ganesan N, Padmanabhan C (2009) Vibration and acoustic response of a composite plate with inherent material damping in a thermal environment. J Sound Vib 320:322–338. https://doi.org/10.1016/j.jsv.2008.08.013
27. Li Q, Iu VP, Kou KP (2009) Three-dimensional vibration analysis of functionally graded material plates in thermal environment. J Sound Vib 324:733–750. https://doi.org/10.1016/j.jsv.2009.02.036
28. Viola E, Tornabene F, Fantuzzi N (2013) Generalized differential quadrature finite element method for cracked composite

structures of arbitrary shape. Compos Struct 106:815–834. https://doi.org/10.1016/j.compstruct.2013.07.034

29. Natarajan S, Chakraborty S, Ganapathi M, Subramanian M (2014) A parametric study on the buckling of functionally graded material plates with internal discontinuities using the partition of unity method. Eur J Mech A/Solids 44:136–147. https://doi.org/10.1016/j.euromechsol.2013.10.003

30. Ansari R, Ashrafi MA, Pourashraf T, Sahmani S (2015) Vibration and buckling characteristics of functionally graded nanoplates subjected to thermal loading based on surface elasticity theory. Acta Astronaut 109:42–51. https://doi.org/10.1016/j.actaastro.2014.12.015

31. Yang S, Chen W (2015) On hypotheses of composite laminated plates based on new modified couple stress theory. Compos Struct 133:46–53. https://doi.org/10.1016/j.compstruct.2015.07.050

32. Dastjerdi S, Akgöz B (2018) New static and dynamic analyses of macro and nano FGM plates using exact three-dimensional elasticity in thermal environment. Compos Struct 192:626–641. https://doi.org/10.1016/j.compstruct.2018.03.058

33. Avcar M (2016) Effects of material non-homogeneity and two parameter elastic foundation on fundamental frequency parameters of Timoshenko beams. Acta Phys Pol A 130:375–378. https://doi.org/10.12693/APhysPolA.130.375

34. Chen W, Li X (2014) A new modified couple stress theory for anisotropic elasticity and microscale laminated Kirchhoff plate model. Arch Appl Mech 84:323–341. https://doi.org/10.1007/s00419-013-0802-1

35. Movassagh AA, Mahmoodi MJ (2017) A micro-scale modeling of Kirchhoff plate based on modified strain-gradient elasticity theory. Eur J Mech/A Solids 40:50–59. https://doi.org/10.1016/j.euromechsol.2012.12.008

36. Kim J, Reddy JN (2015) A general third-order theory of functionally graded plates with modified couple stress effect and the von Kármán nonlinearity: theory and finite element analysis. Acta Mech 226:2973–2998. https://doi.org/10.1007/s00707-015-1370-y

37. Mindlin RD, Eshel NN (1968) On first strain-gradient theories in linear elasticity. Int J Solids Struct 4:109–124. https://doi.org/10.1016/0020-7683(68)90036-X

38. Papargyri-Beskou S, Beskos DE (2007) Static, stability and dynamic analysis of gradient elastic flexural Kirchhoff plates. Arch Appl Mech 78:625–635. https://doi.org/10.1007/s00419-007-0166-5

39. Papargyri-beskou S, Giannakopoulos AE, Beskos DE (2010) Variational analysis of gradient elastic flexural plates under static loading. Int J Solids Struct 47:2755–2766. https://doi.org/10.1016/j.ijsolstr.2010.06.003

40. Mousavi SM, Paavola J (2014) Analysis of plate in second strain gradient elasticity. Arch Appl Mech 84(8):1135–1143. https://doi.org/10.1007/s00419-014-0871-9

41. Akgöz B, Civalek Ö (2013) Modeling and analysis of micro-sized plates resting on elastic medium using the modified couple stress theory. Meccanica 48:863–873. https://doi.org/10.1007/s11012-012-9639-x

42. Akgöz B, Civalek Ö (2015) A microstructure-dependent sinusoidal plate model based on the strain gradient elasticity theory. Acta Mech 226:2277–2294. https://doi.org/10.1007/s00707-015-1308-4

43. Tsiatas GC (2009) A new Kirchhoff plate model based on a modified couple stress theory. Int J Solids Struct 46:2757–2764. https://doi.org/10.1016/j.ijsolstr.2009.03.004

44. Tsiatas GC, Yiotis AJ (2009) A microstructure-dependent orthotropic plate model based on a modified couple stress theory. WIT Trans State Art Sci Eng 34:1755–8336. https://doi.org/10.2495/978-1-84564

45. Tsiatas GC, Yiotis AJ (2015) Size effect on the static, dynamic and buckling analysis of orthotropic Kirchhoff-type skew microplates based on a modified couple stress theory: comparison with the nonlocal elasticity theory. Acta Mech 226:1267–1281. https://doi.org/10.1007/s00707-014-1249-3

46. Yin L, Qian Q, Wang L, Xia W (2010) Vibration analysis of microscale plates based on modified couple stress theory. Acta Mech Solida Sin 23:386–393. https://doi.org/10.1016/S0894-9166(10)60040-7

47. Ebrahimi F, Barati MR (2016) Thermal buckling analysis of size-dependent FG nanobeams based on the third-order shear deformation beam theory. Acta Mech Solida Sin 29:547–554. https://doi.org/10.1016/S0894-9166(16)30272-5

48. Akgöz B, Civalek Ö (2013) Buckling analysis of functionally graded microbeams based on the strain gradient theory. Acta Mech 224:2185–2201. https://doi.org/10.1007/s00707-013-0883-5

49. Demir Ç, Civalek Ö (2017) On the analysis of microbeams. Int J Eng Sci 121:14–33. https://doi.org/10.1016/j.ijengsci.2017.08.016

50. Mercan K, Civalek Ö (2016) DSC method for buckling analysis of boron nitride nanotube (BNNT) surrounded by an elastic matrix. Compos Struct 143:300–309. https://doi.org/10.1016/j.compstruct.2016.02.040

51. Mercan K, Civalek Ö (2017) Buckling analysis of Silicon carbide nanotubes (SiCNTs) with surface effect and nonlocal elasticity using the method of HDQ. Compos Part B Eng 114:34–45. https://doi.org/10.1016/j.compositesb.2017.01.067

52. Mercan K, Numanoglu HM, Akgöz B, Demir C, Civalek (2017) Higher-order continuum theories for buckling response of silicon carbide nanowires (SiCNWs) on elastic matrix. Arch Appl Mech 87:1797–1814. https://doi.org/10.1007/s00419-017-1288-z

53. Numanoğlu HM, Akgöz B, Civalek Ö (2018) On dynamic analysis of nanorods. Int J Eng Sci 130:33–50. https://doi.org/10.1016/j.ijengsci.2018.05.001

54. Gao XL, Zhang GY (2016) A non-classical Kirchhoff plate model incorporating microstructure, surface energy and foundation effects. Contin Mech Thermodyn 28:195–213. https://doi.org/10.1007/s00161-015-0413-x

55. Gupta A, Jain NK, Salhotra R, Joshi PV (2015) Effect of microstructure on vibration characteristics of partially cracked rectangular plates based on a modified couple stress theory. Int J Mech Sci 100:269–282. https://doi.org/10.1016/j.ijmecsci.2015.07.004

56. Gupta A, Jain NK, Salhotra R, Rawani AM, Joshi PV (2015) Effect of fibre orientation on non-linear vibration of partially cracked thin rectangular orthotropic micro plate: an analytical approach. Int J Mech Sci 105:378–397. https://doi.org/10.1016/j.ijmecsci.2015.11.020

57. Wu Z, Ma X (2016) Dynamic analysis of submerged microscale plates: the effects of acoustic radiation and viscous dissipation Subject Areas. Proc R Soc A 472:20150728

58. Soni S, Jain NK, Joshi PV (2019) Vibration and deflection analysis of thin cracked and submerged orthotropic plate under thermal environment using strain gradient theory. Nonlinear Dyn 96(2):1575–1604. https://doi.org/10.1007/s11071-019-04872-3

59. Szilard R (2004) Theories and applications of plate analysis. Wiley, Hoboken. https://doi.org/10.1002/9780470172872

60. Mallick PK (2007) Fibre-reinforced composites: materials, manufacturing and design, 3rd edn. CRC Press, Taylor and Francis Group, Boca Raton

61. Joshi PV, Gupta A, Jain NK, Salhotra R, Rawani AM, Ramtekkar GD (2017) Effect of thermal environment on free vibration and buckling of partially cracked isotropic and FGM micro plates based on a non classical Kirchhoff's plate theory: an analytical approach. Int J Mech Sci 131:155–170. https://doi.org/10.1016/j.ijmecsci.2017.06.044

62. Gupta A, Jain NK, Salhotra R, Joshi PV (2018) Effect of crack location on vibration analysis of partially cracked isotropic and

FGM micro-plate with non-uniform thickness: an analytical approach. Int J Mech Sci 145:410–429. https://doi.org/10.1016/j.ijmecsci.2018.07.015

63. Joshi PV, Jain NK, Ramtekkar GD (2015) Analytical modelling for vibration analysis of partially cracked orthotropic rectangular plates. Eur J Mech A/Solids 50:100–111. https://doi.org/10.1016/j.euromechsol.2014.11.007

64. Bose T, Mohanty AR (2013) Vibration analysis of a rectangular thin isotropic plate with a part-through surface crack of arbitrary orientation and position. J Sound Vib 332:7123–7141. https://doi.org/10.1016/j.jsv.2013.08.017

65. Altan SB, Aifantis EC (1992) On the structure of the mode III crack-tip in gradient elasticity. Scr Metall Mater 26:319–324. https://doi.org/10.1016/0956-716X(92)90194-J

66. Park SK, Gao XL (2006) Bernoulli–Euler beam model based on a modified couple stress theory. J Micromech Microeng 16:2355–2359. https://doi.org/10.1088/0960-1317/16/11/015

67. Yang F, Chong CM, Lam DCC, Tong P (2002) Couple stress based strain gradient theory for elasticity. Int J Solids Struct 39:2731–2743. https://doi.org/10.1016/S0020-7683(02)00152-X

Publisher's Note Springer Nature remains neutral with regard to jurisdictional claims in published maps and institutional affiliations.